

# **Neural Network Classification for High Concentration Ethanol in a Multi Sensor Array Electronic Nose**

A Thesis

Presented to

The Faculty of Graduate Studies

of

The University of Guelph

by

Robert L. Littel

In partial fulfillment of requirements

for the degree of

Masters of Applied Science

In

Engineering Systems and Computing

Guelph, Ontario, Canada

© Robert Littel, 2013

## **Abstract**

### **Neural Network Classification for High Concentration Ethanol in a Multi Sensor Array Electronic Nose**

Robert Littel

University of Guelph, 2013

Advisors:

Dr. Radu Muresan

Dr. Simon X. Yang

An electronic nose was designed to investigate the chemical properties of high concentration Ethanol spirits. The hardware was custom designed, and fabricated to classify spirits with 12 MOS sensors for further analysis with a neural network. Electronic noses have been used for quality control with various foods and beverages in the past. Methods for classification and post processing techniques have varied from numerous publications. The popular methods used in the industry have been presented and their corresponding effectiveness has been analyzed. A systematic procedure has been created which can be used to recreate results for future sample collections. Seven unique features were extracted from 7 sensors that recorded time dependant chemical responses in a controlled environment. The 49 features were used as the inputs into a 45 hidden node middle layer, 3 output, back propagating neural network. This network was able to classify 5  $\mu$ L samples of mixed concentrations of Ethanol, Ethyl Acetate and Isopropyl Alcohol to within 12.5% accuracy.

## **Dedication**

*To my parents: Bob and Barb Littel.*

## **Acknowledgements**

I would like to acknowledge numerous individuals throughout the course of my study at Guelph. Many thanks go to Dr. Radu Muresan for his support and guidance and ultimately for the opportunity to work on this project. I would also like to thank my co-advisors Dr. Simon X. Yang and Dr. Stefano Gregori for their recommendations and guidance throughout my studies. I would like to thank my partner Mark Lieberman for all of his time and efforts for helping accomplish everything we did. I would like to show my gratitude towards Mr. David Doyle, and Dr. Sapna Sharma at Pernod-Ricard for the opportunity to work on this project and for their company's financial contributions in supporting further scientific research into the electronic nose industry.

Financial support for this project was granted by the Ontario Centres of Excellence (OCE) and from Pernod-Ricard (Project No. TP-SW-11168-11).

# Table of Contents

Dedication .....	ii
Acknowledgements .....	iii
List of Tables .....	viii
List of Figures .....	ix
1 Introduction.....	1
1.1 Thesis Objective .....	2
1.2 Contributions of this Thesis .....	3
1.3 Organization of Thesis .....	4
2 Background .....	5
2.1 E-Nose Systems and the Human Nose .....	7
2.1.1 Sensor Array .....	7
2.1.2 Computational Unit.....	8
2.1.3 Structural Design.....	9
2.2 Spirits (Whisky) .....	9
2.2.1 Ethanol .....	11
2.2.2 Ethyl Acetate.....	12
2.2.3 Ethyl Butyrate .....	13
2.2.4 Propylene Glycol.....	14
2.2.5 Vanillin.....	15

2.2.6	Isopropyl Alcohol .....	16
2.2.7	Summary .....	17
2.3	Sensors .....	17
2.3.1	FiS Gas Sensors .....	19
2.3.2	Figaro Gas Sensors.....	20
2.4	Neural Networks .....	22
2.4.1	Nomenclature .....	23
2.4.2	Network Creation.....	25
2.4.3	Notes .....	32
2.5	Summary .....	32
3	Literature Survey .....	33
3.1	Known Uses of Electronic Noses.....	33
3.2	Data Feature Extraction Methods.....	34
3.3	Hardware implementation.....	36
3.4	Summary .....	37
4	E-Nose Box Design .....	39
4.1	Dimensions .....	40
4.2	Heater Design.....	42
4.3	Fan Mount Design.....	49
4.4	Airline Filtration.....	51

4.5	Summary of the Overall Design.....	52
5	Experimental Procedures and Trial Results.....	55
5.1	System Setup.....	55
5.1.1	System Tab.....	57
5.1.2	Capture Tab.....	57
5.1.3	Processes Tab.....	58
5.1.4	Reaching steady state.....	59
5.2	Sample Collection Methods.....	61
5.2.1	Procedure 1: Open Vial Heating Chamber.....	61
5.2.2	Procedure 2: Immediate Sample Flow.....	65
5.2.3	Procedure 3: No Air Flow during Baseline Recordings.....	66
5.2.4	Procedure 4: No air flow when reading a trapped sample.....	68
5.3	Fan Speed and Air Flow Rate.....	69
5.4	Summary.....	70
6	Results.....	71
6.1	Procedure.....	71
6.2	Sample Collection Accuracy.....	74
6.3	Feature Extraction.....	80
6.4	Neural Network Classification.....	81
6.5	Summary.....	89

7	Conclusion .....	90
7.1	Future Work .....	91
	Bibliography.....	92
	Appendix A – 2D Drawings .....	98
	Appendix B – Sample Initialization Conditions .....	102



## List of Tables

Table 1: Ethanol Properties Summary .....	12
Table 2: Ethyl Acetate Properties .....	13
Table 3: Ethyl Butyrate Properties.....	14
Table 4: Propylene Glycol Properties .....	15
Table 5: Vanillin Properties .....	16
Table 6: Isopropyl Alcohol Properties .....	16
Table 7: Chemical Summary Table .....	17
Table 8: Final Prototype Major Component List .....	40
Table 9: Vial Heater Top Section Part List.....	44
Table 10: Vial Heater Bottom Section Part List .....	46
Table 11: Motor Fan Mount Part List .....	50
Table 12: Sample Comparison Details .....	79
Table 13: Feature Extraction Table.....	81
Table 14: Learning Rate Adjustment .....	82
Table 15: Neural network output classification for 5 samples .....	83
Table 16: Neural Network Architecture Results.....	85
Table 17: Neural Network Epoch Summary Table.....	85
Table 18: Neural Network Hidden Node Summary Table .....	86
Table 19: Classification Error for 1000, 2000, and 3000 epochs for Individual Outputs.....	87
Table 20: Sample Initialization Conditions Part 1 .....	102
Table 21: Sample Initialization Conditions Part 2 .....	103
Table 22: Sample Initialization Conditions Part 3 .....	104

## List of Figures

Figure 1: Pernod-Ricard Sample Array .....	10
Figure 2: Ethanol - Ball and Stick Molecular Structure .....	12
Figure 3: Ethyl Acetate - Ball and Stick Molecular Structure .....	13
Figure 4: Ethyl Butyrate - Ball and Stick Molecular Structure .....	14
Figure 5: Propylene Glycol - Ball and Stick Molecular Structure .....	15
Figure 6: Vanillin - Ball and Stick Molecular Structure .....	16
Figure 7: Isopropyl Alcohol - Ball and Stick Molecular Structure.....	16
Figure 8: FiS SB15 Configuration [22] .....	19
Figure 9: FiS SB15 Sensitivity Characteristics [22] .....	20
Figure 10: TGS2610-C00 and TGS2610-D00 [23] .....	21
Figure 11: TGS2610-C00 Sensitivity Characteristics [23].....	22
Figure 12: TGS2610-D00 Sensitivity Characteristics [23].....	22
Figure 13: Simple Neural Network.....	23
Figure 14: Structure of fully connected three-layer back propagation network [25] .....	35
Figure 15: Electronic Nose Final Prototype.....	39
Figure 16: Vial Heater Top Section .....	44
Figure 17: Vial Heater - Bottom Section .....	46
Figure 18: Vial Heater System Final Prototype .....	48
Figure 19: Motor Mount Exploded View .....	50
Figure 20: Airline Filtration System- Internal .....	52
Figure 21: Airline Filtration System - All.....	52
Figure 22: Final Design Exploded .....	53

Figure 23: Electronic Nose Setup .....	54
Figure 24: Electronic Nose Internal Chamber .....	54
Figure 25: Berry Punch Operators Interface - Resistor Select.....	56
Figure 26: A 5 $\mu$ L Ethanol 20% ABV sample preheated at 80°C for 120 seconds sample response with 120 second data recording .....	63
Figure 27: A 5 $\mu$ L Ethanol 20% ABV sample preheated at 80°C for 135 seconds sample response with 180 second data recording .....	63
Figure 28: A 5 $\mu$ L Ethanol 20% ABV sample preheated at 80°C for 150 seconds sample response with 180 second data recording .....	64
Figure 29: A 5 $\mu$ L Ethanol 20% ABV sample preheated at 80°C for 165 seconds sample response with 180 second data recording .....	64
Figure 30: A 5 $\mu$ L Ethanol 20% ABV sample released into the chamber immediately and recorded until no response found.....	66
Figure 31: No air flow when reading sample: A 5 $\mu$ L Sample with Ethanol at 20% ABV for 360 seconds.....	67
Figure 32: A 5 $\mu$ L Sample with Ethanol at 20% ABV response when in chamber 120 seconds and no airflow. ....	69
Figure 33: Sensor 2 Comparable Sample Data Recordings - Resistance .....	76
Figure 34: Sensor 3 Comparable Sample Data Recordings - Resistance .....	77
Figure 35: Sensor 3 Comparable Sample Data Recordings - Normalized Conductance.....	78
Figure 36: Neural Network Architecture .....	86
Figure 37: Neural Network Output Error Graph.....	88
Figure 38: 2D Drawing - Motor Bottom Support Block.....	98

Figure 39: 2D Drawing - Motor Top Support Block ..... 99

Figure 40: 2D Drawing - Vial Heater Bottom Section Block..... 100

Figure 41: 2D Drawing - Vial Heater top Section Block..... 101

# Chapter 1

## 1 Introduction

Quality control for foods and beverages has become both exceedingly important and highly regulated due to the massive quantities of a product that can be produced in today's autonomous world. The quality of a product can be determined through numerous classification methods and also through automated processing techniques. The aroma produced by a product can make a large difference in value which influences the purchasing decision. Throughout history, humans have used their own sense of smell as the most popular method to interpret and classify an odor. In the food industry, a panel of judges takes a long time to be trained and when a more scientific approach is taken, gas chromatography is often the method utilized for analysis. An electronic nose is a modern approach to classify an odor by registering the output of a smell as a digital signature or fingerprint. Electronic noses operate by using an array of sensors to record the response of a chemical and then classify the reaction through advanced signal processing techniques. The array of sensors used can dramatically vary in size and are often MOS gas sensors which are popular due to their low cost, selectivity, and ease of fabrication.

The alcohol beverage industry sold close to \$21 billion in Canada during the 2012 fiscal year (ending March 31, 2012) which was an increase of 3% from the previous year. Approximately 25% of this market's revenue is accounted for by the sale of spirits and the Government of Canada Committee has also recommended that the country should invest towards innovation and research and development in this industry [1]. These records and statements produced by the Canadian government create a potential market for an electronic nose to operate in. There is a long aging process for spirits where the headspace of a barrel offers a unique

opportunity such that an electronic nose could be used to examine it. Whisky is typically brewed in wood barrels constructed from different types of trees and this will slightly alter the resulting output. The unbiased precision by an electronic nose can inform brew masters when the blend is ready for the next stage of the bottling process by detecting levels of specific compounds that increase with time such as Acetaldehyde and Ethyl Acetate [2].

The value of this industry also leads to illegal operations where fake and counterfeit products are found throughout the world and are sold to consumers under an established brand name. Consumers purchasing these ‘imitation’ products may become upset with the big name brands which can damage the reputation of the companies. These counterfeit bottles are not produced with the same quality, and are typically brewed with a self made recipe consisting of unsettling flavors and possible contaminants such as Ethylene Glycol which could harm a consumer [3]. An electronic nose could serve as a portable solution to detecting the quantities found in such products and may help lead to the reduction in counterfeit alcohol.

## **1.1 Thesis Objective**

This work is an attempt to create an electronic nose prototype to investigate the analysis of high concentration spirits. A 12 MOS sensor custom fabricated electronic nose was developed to attempt to classify the off compounds associated with Whisky and other popular alcoholic beverages. This classification will be accomplished through signal response feature extraction and a back propagating neural network. Mixed concentrations of Ethanol, Ethyl Acetate, and Isopropyl Alcohol will be analyzed for classification.

## 1.2 Contributions of this Thesis

The following is a list summarizing the main accomplishments of this thesis:

- A physical lab bench electronic nose has been created as a prototype from US Patent (Number 20130061692A1) which features an air chamber, custom fabricated vial heating chamber, custom fabricated fan mount, and a baseline air ventilation system [4].
- Feature extraction methods to process the data from sample collection using MATLAB have been created.
- Five primary systematic lab experiments were designed to optimize the data collection process. These methods were thoroughly tested against multiple sample sizes and chemicals.
- The data collected required a baseline manipulation analysis to create a fair comparison of the data collected.
- A back propagating neural network was made to classify mixed concentrations of chemicals. The network architecture was created by cycling through different architectures and the design with the lowest error was used.

### **1.3 Organization of Thesis**

This thesis has been organized into seven chapters to cover all necessary steps from the development of the electronic nose through to the classification stage.

*Chapter 1* is about the overview of this thesis. It provides a basic introduction into what has been accomplished.

*Chapter 2* provides background information on available electronic nose systems and from where their advancements have been inspired. This section also describes background information on the chemicals analyzed, the sensors being used, and an overview of how a back propagation neural network functions.

*Chapter 3* presents a literature review on the available electronic nose systems, an investigation into common classification methods as well as common electronic nose hardware.

*Chapter 4* describes the process of the creation of the electronic nose. It shows the design process of the final prototype as well as the physical properties of the final design used for data collection.

*Chapter 5* is an overview on how to set up the electronic nose for sample collection and outlines multiple procedures that were investigated for data collection.

*Chapter 6* features the final procedure used to collect results as well as the neural network classification results from this thesis.

*Chapter 7* concludes this thesis with closing remarks and recommendations for future work.



## Chapter 2

### 2 Background

Electronic noses (E-nose) are commonly defined as “*An instrument which comprises an array of electronic chemical sensors with partial specificity and an appropriate pattern recognition system, capable of recognizing simple or complex odors.*”[5].

The smell of a food or beverage can play a very important role when determining how much one enjoys what they are consuming. Wines for example, are commonly evaluated through a series of tests amongst a panel of judges to determine the quality of the wine; one of these tests ranks the smell. Humans take a long time to become accustomed to what the actual smell of the beverage should correctly be, and thus it can take a very long time to train an expert panel of judges. Some chemicals found in beverages are found in such a small quantity that only a few people are actually able to correctly smell them or in some cases not at all. To intensify this problem, judges can become easily influenced by subjective factors when giving an analysis [6].

Electronic noses offer a solution to this evaluation and are becoming more popular in the food and beverage industry. They are able to accurately classify many characteristics about the product being analyzed. Mimicking the olfactory system with a series of sensors can consistently label the subject matter without any bias. These electronic systems require an abundance of sample data to be able to properly work in the field and also require a significant amount of training. There have been many signal processing methods developed that have been applied to work with electronic noses and some continually produce better results than others.

Using an electronic nose in an active biological system is difficult due to the changing nature of the aging products and the sensors producing non-linear results [7]. However, detection limits as low as 2~5 ppm have been reported using olfactory receptor based sensors [7].

The sensors used on an electronic nose are traditionally not selective which creates the inherent problem of being able to correctly classify specific beverages. Starting steps for classification can simply be if the product is good or bad. The outcome can be determined by taking a small sample from a batch and using the characteristic response of the sensors to classify the food / beverage [6][8].

When collecting information for beers, there is a set of standards under the Polish Standards, “Beer, Sampling and testing methods. PN-74 A-79903” such that a beer can be properly evaluated by [6]:

- Clarity
- Color
- Bitterness
- Extract in original wort
- Apparent extract
- Real extract
- Concentration of alcohol in beer
- Real degree of fermentation
- Apparent ferment ability
- Ph
- Concentration of carbon dioxide in beer
- Beer acidity

Although these are not all qualities that an electronic nose can individually detect, they are qualities that can help train and identify a specific product.

Some companies publish their information on quality whereas other information can be found from university websites such as the 'Olfactory Receptor Database' which is developed and maintained by the Shepherd Lab, Yale University, School of Medicine, USA [7]. Liquid chromatograms can also be used to breakdown the compounds of the beverage which can help determine the characteristics of the subject matter and to reinforce the validity of the result [6] .

However, a problem can occur when too much information is presented to be analyzed. Some of the information may not help a system at all when trying to determine the answer to a specific problem, yet that quality may be important when determining another characteristic about the testing matter.

In recent years there have been a number of publications where an electronic nose was used for quality analysis and the best method for how to determine the desired quality can change from product to product. Numerous articles have published their findings using soft computing methods which will be further analyzed and presented in Section 6.

## **2.1 E-Nose Systems and the Human Nose**

Electronic noses are a minimalistic approach for mimicking a human nose in an electronic form. They are produced in many different shapes and sizes with the most advanced ones being permanent lab structures that are not easily transported for field work. The primary components found in a common electronic nose feature: a sensor array, computational unit, and the structural design.

### **2.1.1 Sensor Array**

A human nose features between 5 and 10 million olfactory neurons inside the top of the nasal passage. These neurons have small hair like projections called cilia which help amplify the

surface area of this section of the body. These neurons have different olfactory receptors which are encoded by different genes. It is considered that the human nose is able to detect more than 10,000 different smells and this can be accomplished by using specific combinations of receptors to determine what is actually being smelt[9].

An electronic nose attempts to mimic this system by having an array of sensors used to detect an odorant. Due to the physical size and computational power required to classify an odor, the array size for an electronic nose has dramatically fewer sensors than that of a human nose. There is not a specific sensor that exists for every known chemical and thus electronic noses are typically designed with a certain class of odor in mind. Sensors in production have a wide variety of sensitivity and thus it is important to consider the strength of the odor attempting to be classified.

### **2.1.2 Computational Unit**

The human brain does a remarkable job at making intelligent decisions and classifying objects. It can learn by repetition and has the ability to detect minute differences in the senses it is exposed to. The neurological calculations that happen in the brain are still not fully understood and model day computers still cannot match the brain's high performance levels.

The sensors used in an electronic nose require that the signal output be analyzed to produce a classification result. Sensor output can differentiate by design, but usually a time dependent response from each sensor is stored as a data array in a database where the known components of the sample being analyzed are also provided. Similar to the human brain, a computer needs to 'learn' about new smells and this is determined by feature extraction from the resulting sensors. Supervised learning methods are common approaches to classification techniques.

### 2.1.3 Structural Design

Minimizing the variables in an environment can lead to more consistent and accurate results. An enclosed structure housing the sensors can help the system by having a common known baseline and minimizing external unknown variables. This structure will typically feature many side qualities to recreate a consistent environment such as temperature and humidity control. Most sensors will produce a different response when the temperature or humidity is different, and some sensors will simply not work if the humidity level is too low. After each 'sample', the environment should be cleaned out such that the previous odor is removed until the normal 'baseline' conditions are met again. This process is typically accomplished by flushing out the chamber with a known reference gas.

## 2.2 Spirits (Whisky)

Spirits have been a subject of analysis in previous electronic nose devices; however they have proven to be difficult to work with due to the high concentration of Ethanol. Successful classifications have been made with Whisky and Brandy [10]. The primary focus and identifiable feature in spirits is Ethanol. There are also many off-compounds which are found in the final product which exist because they are 'immune' to filtration and the distilling process. Given a breakdown of the component analysis from a fractioning column by Pernod Ricard, specific compounds have been further investigated for this thesis. The main criteria for further investigation of the provided spirits would resolve around the following chemical traits:

- 1) **Concentration**; amount of the chemical that is found in common spirits.
- 2) **Reoccurrence**; likelihood that the compound exists in a majority of spirits.
- 3) **Chemical Properties**; identifiable traits of the chemical that influence performance.
- 4) **Vapor Pressure**; related to the tendency of particles to escape from a liquid or solid.

- 5) **Smell Potency**; how easy is it for a human to detect the compound?
- 6) **Accessibility**; how easy it is to acquire pure samples?
- 7) **Sensor Response**; likelihood that the sensors will be able to detect the compound.

For the above reasons, five chemical compounds were investigated as well as an additional inexpensive alcohol to reference. The five chemical compounds investigated were; Ethanol, Ethyl Acetate, Ethyl Butyrate, Propylene Glycol, and Vanillin. These five chemicals were given to us to investigate by Pernod-Ricard in known concentrations for analysis and are pictured below in Figure 1. Isopropyl Alcohol was chosen as an inexpensive easily acquirable alcohol for referencing. The following is the background information on each chemical.



Figure 1: Pernod-Ricard Sample Array

### 2.2.1 Ethanol

Ethanol is also called ethyl alcohol; it is pure alcohol and found in any alcoholic beverage. Most alcoholic drinks range from 3% alcohol by volume (ABV), up to 90% ABV. In Canada, if a beverage contains more than or equal to 1.1% ABV it is considered an alcoholic beverage [1]. For this reason it is an essential starting point to investigate for an electronic nose designed for spirit analysis. It has a very potent and recognizable smell. When a governing board of spirit testers smells a high ABV spirit, the desired concentration is 20% ABV. This amount is considered by experts and associations to be the best to use because the potent smell of ethanol is not too overpowering to block the other odors, and allows for the largest bouquet of smells to be sensed[11][12][13].

The structural formula of Ethanol is  $C_2H_6O$  and physically appears at the molecular level as shown in Figure 2 below. Not only is this compound found in every spirit, but it has a lower boiling point than water at 78.5 °C, and thus could be evaporated into a sensing chamber or separate exhaust collection chamber [14].

The vapor pressure is an important feature because it is desirable as an operator to understand how easy the particles will escape from a solution. Higher temperatures will result in a higher vapor pressure. The vapor pressure for Ethanol is 5.95 kPa (43.7mmHg) at 20 °C. The molar mass of Ethanol is 46.07 g/mol and it is important to know such that one can calculate concentrations found in samples in terms of parts per million (ppm)[14].

Ethanol is very easy to acquire, it is a very popular solution that is studied and is not too expensive to synthesis or acquire. It is extremely likely that Ethanol will be detected in the

designed electronic nose, given that the sensors selected for the electronic nose were chosen to detect it. A summary of the above information is listed below in Table 1.

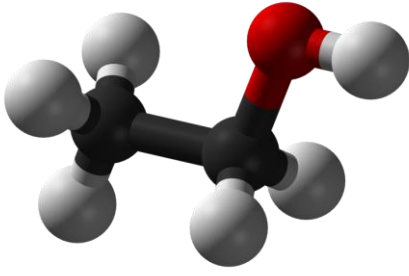
Ethanol Properties		
 <p>Figure 2: Ethanol - Ball and Stick Molecular Structure</p>	<b>Chemical</b>	Ethanol (C <sub>2</sub> H <sub>6</sub> O)
	<b>Boiling Point</b>	78.5°C
	<b>Vapor Pressure</b>	5.95 kPa (43.7mmHg) at 20°C
	<b>Molar Mass</b>	$M = 46.06 \frac{g}{mol}$
	<b>Odor</b>	Strong
	<b>Taste</b>	Bitter

Table 1: Ethanol Properties Summary

### 2.2.2 Ethyl Acetate

Ethyl Acetate is a colorless liquid that smells similar to Ethanol, but also has a sweet smell similar to that of pear drops. Its chemical formula is C<sub>4</sub>-H<sub>8</sub>-O<sub>2</sub> and appears at the molecular level as shown in Figure 3 below. The boiling point of this compound is 77°C and the vapor pressure is 12.4 kPa (73.911mmHg) at 20°C which has similar characteristics to Ethanol [15]. The molar mass is 88.11 g/mol. Considering that Ethyl Acetate is actually the ester of Ethanol, this compound should theoretically be easily detectable by the sensors designed to detect straight Ethanol. Ethyl Acetate is typically manufactured on a large scale and used as a solvent which makes this compound easily accessible and cheap to purchase. A summary of the above information is listed below in Table 2



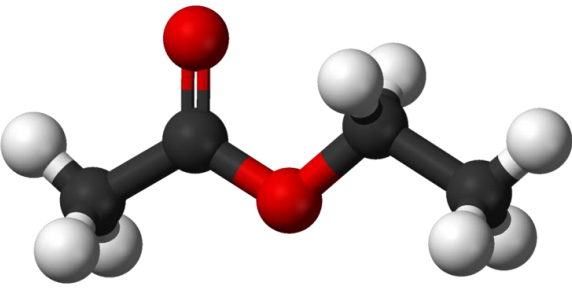
Ethyl Acetate Properties		
 <p>Figure 3: Ethyl Acetate - Ball and Stick Molecular Structure</p>	<b>Chemical</b>	Ethyl Acetate (C <sub>4</sub> -H <sub>8</sub> -O <sub>2</sub> )
	<b>Boiling Point</b>	77°C
	<b>Vapor Pressure</b>	12.4 kPa (73.911mmHg) at
	<b>Pressure</b>	20°C
	<b>Molar Mass</b>	$M = 88.1 \frac{g}{mol}$
	<b>Odor</b>	Strong

Table 2: Ethyl Acetate Properties

### 2.2.3 Ethyl Butyrate

Ethyl Butyrate has a very potent and recognizable odor that smells like candy and pineapple. It is very commonly used in the food and beverage industries as artificial flavoring. With alcoholic beverages, it is commonly used in martinis and daiquiris. This flavor is very cheap to purchase and thus easily accessible. The chemical formula is CH<sub>6</sub>-H<sub>12</sub>-O<sub>2</sub> and the molecular structure is shown below in Figure 4.

The boiling point is 120°C, and the vapor pressure is 1.7 kPa (11.3 mmHg) at 20°C which allows Ethyl Butyrate particles to escape from the solution very easily and should be very easy to smell at room temperature. Although it is very easy for a human to sense this chemical, it is questionable how easy if at all the Ethanol sensors will detect this compound. Due to this chemicals popularity, it should be heavily investigated by the electronic nose. The molar mass is 116.16 g/mol [16]. A summary of the above information is listed below in Table 3.

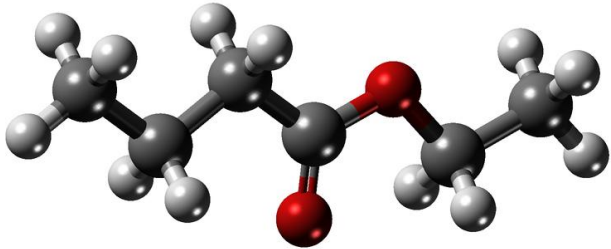
Ethyl Butyrate Properties		
 <p>Figure 4: Ethyl Butyrate - Ball and Stick Molecular Structure</p>	<b>Chemical</b>	Ethyl Butyrate (CH <sub>6</sub> -H <sub>12</sub> -O <sub>2</sub> )
	<b>Boiling Point</b>	120°C
	<b>Vapor Pressure</b>	1.7 kPa (11.3 mmHg) at 20°C
	<b>Molar Mass</b>	$M = 116.16 \frac{g}{mol}$
	<b>Odor</b>	Strong, Candy / Pineapple flavored

Table 3: Ethyl Butyrate Properties

#### 2.2.4 Propylene Glycol

Propylene Glycol is an organic compound that is also a colorless liquid, and is miscible with water. This means that it will form a solution and mix in all proportions with water. One common use of this compound is as a preservative for food. It is created in industrial quantities and thus is not difficult to acquire. It is recognized as safe by the US Food and Drug Administration however there are warnings about nasal ingestion at large quantities. The chemical formula for this compound is C<sub>3</sub>H<sub>8</sub>O<sub>2</sub> and the molecular structure is shown below in Figure 5.

The boiling point for Propylene Glycol is 188°C, the vapor pressure is 0kPa at 20°C (0.129mmHg at 25°C), and the molar mass is 76.1 g/mol [17]. A summary of Propylene Glycol's information is listed below in Table 4. These qualities make this compound appear to be very difficult to sense for many reasons:

- 1) It is miscible in water.
- 2) The boiling point is significantly higher than the limitations of our heating chamber.
- 3) It is considered nearly odorless, and the vapor pressure is extremely low.

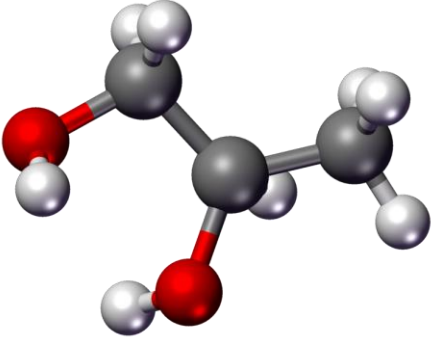
Propylene Glycol Properties		
	<b>Chemical</b>	Propylene Glycol (C <sub>3</sub> H <sub>8</sub> O <sub>2</sub> )
	<b>Boiling Point</b>	188°C
	<b>Vapor Pressure</b>	0kPa at 20°C (0.129mmHg at 25°C)
	<b>Molar Mass</b>	$M = 76.1 \frac{g}{mol}$
	<b>Odor</b>	Nearly odorless

Figure 5: Propylene Glycol - Ball and Stick Molecular Structure

Table 4: Propylene Glycol Properties

### 2.2.5 Vanillin

Vanillin is an organic compound and the primary extract of the vanilla bean, however synthetic Vanillin is more commonly used as a flavoring agent for foods. In its pure form it is a solid, however it can be dissolved into certain solutions. The vanilla flavor is very popular and supply has always exceeded the demand for the natural extract which has lead to this product being rather expensive. Vanillin is regularly used as a substitute because it smells very similar to vanilla; it is used as a flavoring for food products to make them taste creamier. The chemical formula for Vanillin is C<sub>8</sub>H<sub>8</sub>O<sub>3</sub> and the molecular structure is shown below in Figure 6. The boiling point is 285°C and the vapor pressure is so low that it is considered not applicable (approx 1Pa). The molar mass is 152.15g/mol [18]. A summary of the above information is listed below in Table 5.

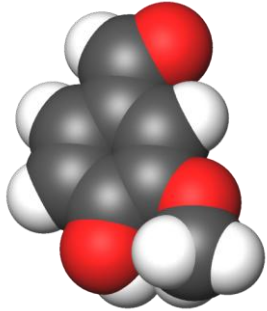
Vanillin Properties		
 <p>Figure 6: Vanillin - Ball and Stick Molecular Structure</p>	<b>Chemical</b>	Vanillin (C <sub>8</sub> H <sub>8</sub> O <sub>3</sub> )
	<b>Boiling Point</b>	285°C
	<b>Vapor Pressure</b>	Not Applicable (approx 1Pa)
	<b>Molar Mass</b>	$M = 152.15 \frac{g}{mol}$
	<b>Odor</b>	Strong – Vanilla flavored

Table 5: Vanillin Properties

### 2.2.6 Isopropyl Alcohol

Isopropyl Alcohol is a chemical compound that is flammable and has a strong odor. It is not safe to drink but is very easily accessible to purchase as rubbing alcohol. It is available to purchase as a 100% pure solution and can be tested in an electronic nose as a comparative alcohol. The chemical formula for this compound is C<sub>3</sub>H<sub>8</sub>O and the molecular structure is shown below in Figure 7. The boiling point is 82.5°C, and the vapor pressure is 4.4 kPa at 20°C. The molar mass is 60.10 g/mol [19]. A summary of this information is listed below in Table 6.

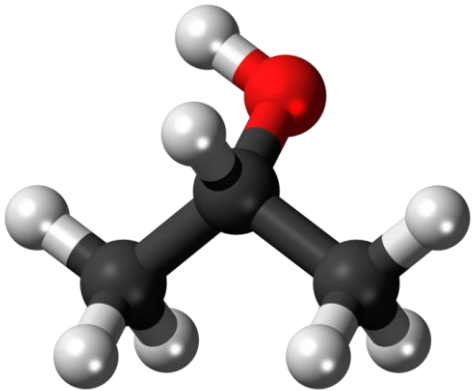
Isopropyl Alcohol Properties		
 <p>Figure 7: Isopropyl Alcohol - Ball and Stick Molecular Structure</p>	<b>Chemical</b>	Isopropyl Alcohol (C <sub>3</sub> H <sub>8</sub> O)
	<b>Boiling Point</b>	82.5°C
	<b>Vapor Pressure</b>	4.4 kPa at 20°C
	<b>Molar Mass</b>	$M = 60.10 \frac{g}{mol}$
	<b>Odor</b>	Strong

Table 6: Isopropyl Alcohol Properties

## 2.2.7 Summary

The following table (Table 7) is a summary table of all the above listed compounds describing their physical and chemical attributes:

Chemical	Boiling Point	Vapor Pressure	Molar Mass	Odor
Ethanol	78.5°C	5.95 kPa at 20°C 43.7mmHg at 20°C	$M = 46.06 \frac{g}{mol}$	Strong
Ethyl Acetate	77°C	12.4 kPa at 20°C 73.91 mmHg at 20°C	$M = 88.1 \frac{g}{mol}$	Strong
Ethyl Butyrate	120°C	1.7 kPa at 20°C 11.3 mmHg at 20°C	$M = 116.16 \frac{g}{mol}$	Strong, Candy / Pineapple flavored
Propylene Glycol	188°C	0kPa at 20°C 0.129mmHg at 25°C	$M = 76.1 \frac{g}{mol}$	Nearly odorless
Vanillin	285°C	Not Applicable (> 1Pa)	$M = 152.15 \frac{g}{mol}$	Strong – Vanilla flavored
Isopropyl Alcohol	82.5°C	4.4 kPa at 20°C	$M = 60.10 \frac{g}{mol}$	Strong

Table 7: Chemical Summary Table

## 2.3 Sensors

The sensors used in an electronic nose are typically chosen to target specific compounds. A large array of various sensors should be able to find different components available in the sample. The most popular type of gas sensors that are used are metal-oxide gas sensors which were first used commercially in the 1960s [20].

MOS sensors usually operate by keeping the sensing surface at a high temperature which is accomplished through an internal heater. By adjusting the electron density at the sensing surface,

the conductance of sensing surface varies making the sensor more or less sensitive to the external gases [21]. The resistance on the surface of the sensor is governed by the concentration of the gas surroundings and the equation:

$$R_s = K[C]^{-\alpha}$$

Where;

- $R_s$  = Electrical resistance of sensor surface
- $K$  = Constant
- $C$  = Gas concentration
- $\alpha$  = Constant dependant on gas type

To find the concentration of a vapor volume for a VOC in the gas chamber from the gas phase concentration the following equation can be used:

$$V_{vap} = \frac{CV_{gc}}{1,000,000}$$

Where;

- $V_{vap}$  = Vapor volume of VOC
- $C$  = Gas phase concentration
- $V_{gc}$  = Gas chamber volume

To find the vapor volume from a liquid for a volatile organic compound (VOC) in the gas chamber, the following equation can be used:

$$V_{vap} = \frac{d_{liq} V_{liq} RT}{MP} * 1,000$$

Where;

- $V_{\text{vap}}$  = Vapor Volume produced (mL)
- $d_{\text{liq}}$  = Density of the liquid VOC
- $V_{\text{liq}}$  = Volume of liquid of VOC (mL)
- $R$  = Ideal gas constant =  $0.08206 \text{ L atm K}^{-1} \text{ mol}^{-1}$
- $T$  = Laboratory Temperature
- $M$  = Molecular weight of VOC
- $P$  = Laboratory pressure

### 2.3.1 FiS Gas Sensors

The FiS gas sensor SB-15 is primarily designed for LP-Gas (propane and butane) detection. It is a tin dioxide semiconductor which features high sensitivity to LP gas, low sensitivity to noise gases, a quick response speed, strong poisoning resistance and a significant low power consumption design (120 mW) [22]. The sensor is shown below in Figure 8.

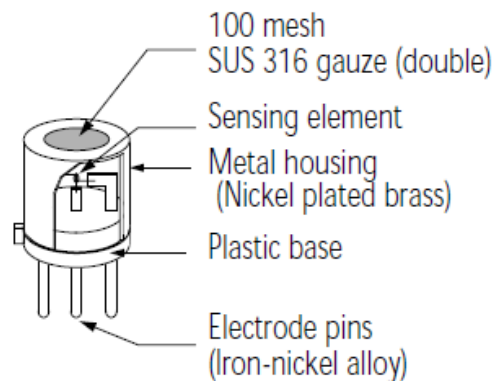


Figure 8: FiS SB15 Configuration [22]

The sensitivity characteristics are displayed in the following graph (Figure 9) which highlights the relationship between the sensor resistances vs. gas concentration. This graph shows logarithmically that the sensor resistance decreases as the concentration of the reference gas increases [22].

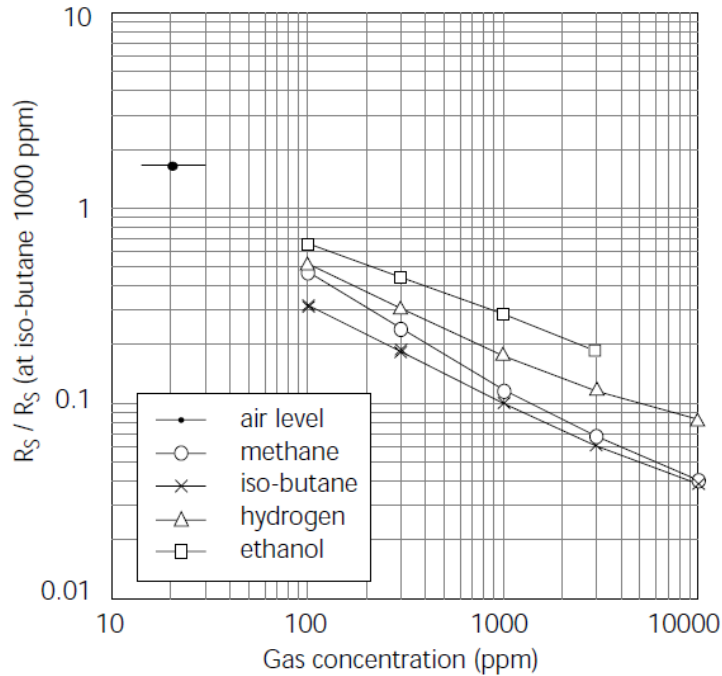


Figure 9: FiS SB15 Sensitivity Characteristics [22]

### 2.3.2 Figaro Gas Sensors

The TGS2610 LP gas sensor is used to detect LP gases. The sensors are manufactured with an ID number which indicates a presorted classification that corresponds to a narrow range of the sensors resistance to Isobutene. This number can help reduce calibration time with the calibrating gases. A load resistor can be interchanged in the circuit to optimize the resolution of the output from the sensor. Figaro has recommended that the load resistor should be equal to the sensors resistance of the target gas;  $R_S / R_L = 1$ [23]. The TGS2610 has proven to be successful in previous electronic nose attempts when analyzing similar alcohols such as Iso Propyl Alcohol and Ethanol [21]. Figure 10 below displays the TGS 2610 C and D.



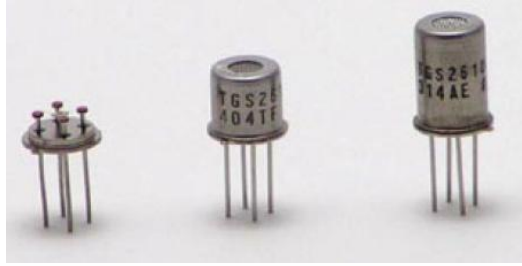
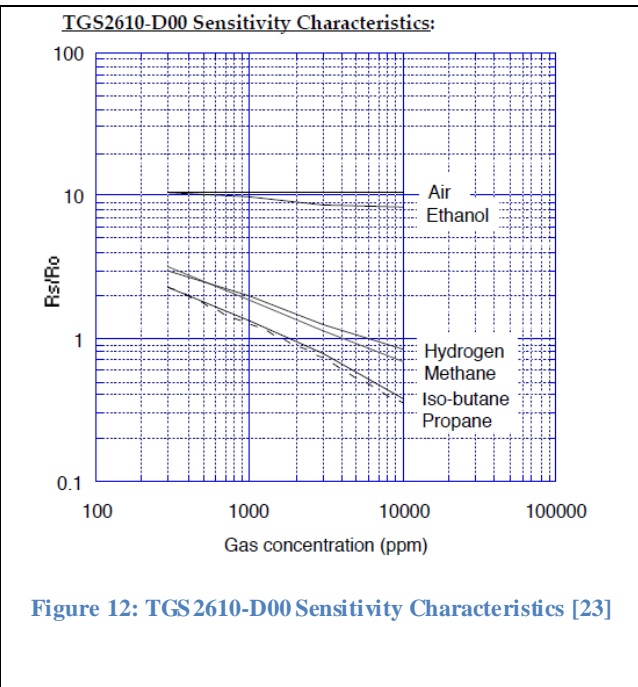
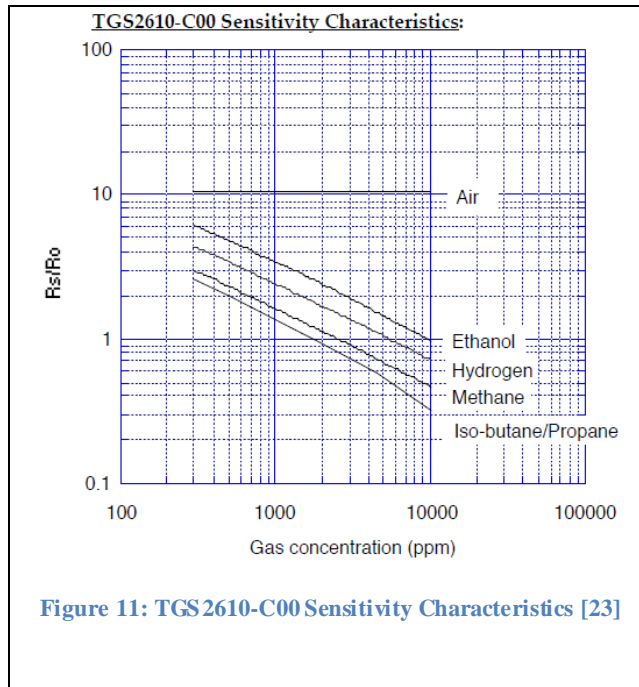


Figure 10: TGS2610-C00 and TGS2610-D00 [23]

These sensors should be stored at room temperature in a clean air environment, where clean air refers to “air free of contaminants, excessive dust, solvent vapors, and etc. Room temperature should be between 20°C and 25°C” [23]. When using the sensor, it is important to preheat the sensor in its environment for 48 hours before using for the first time.

The features of these sensors are that they require low power, have high sensitivity to LP gas and its component gases (e.g. Propane and Butane), have long life, low cost, and operate with a simple electrical circuit. Due to the small size of the sensing chip, it requires a heater that operates at 56 mA. There are two different models of the 2610 which differ in shape but have identical sensitivity to LP gas. The difference is that the TGS2610C is smaller and has a quicker response which makes it more suitable for leak detection. The larger TGS2610D has a filter which helps to reduce the effects of other gases interfering with the response. The filter helps to reduce the effects that alcohol has on the sensor such that this sensor should help to detect off-chemicals in the chamber and has a higher selective response to LP gases [23]. Figure 11 and Figure 12 below show the sensor responses of both the TGS2610C and TGS2610D to various gases. It is clear that the responses between both sensors are very similar as designed.



## 2.4 Neural Networks

Neural networks have become popular in the soft computing field. As the processing power of computers has increased, the complexity and speed in terms of performance has also been improved. This has allowed for more difficult multivariable problems to be solved. They are biologically inspired and feature many different types of architectures which are described using common neurological words. Biologically inspired neural networks are typically now referred to as Artificial Neural Networks (ANN). A main advantage to using a neural network is that they can help solve complex nonlinear problems by detecting patterns in large datasets.

A simple neural network (NN) features three layers; an input layer, hidden layer, and output layer. There has been a lot of research into ideal architecture designs and it has been accepted that a 3 layer network can solve any classification problem because it has sufficient degrees of freedom [24][25]; however a NN could theoretically contain an infinite number of hidden layers.

The following image (Figure 13) is the standard architecture of an ANN such that the input layer is connected to the hidden layer by a set of weights, and the hidden layer is connected to the output layer by its own unique set of weights:

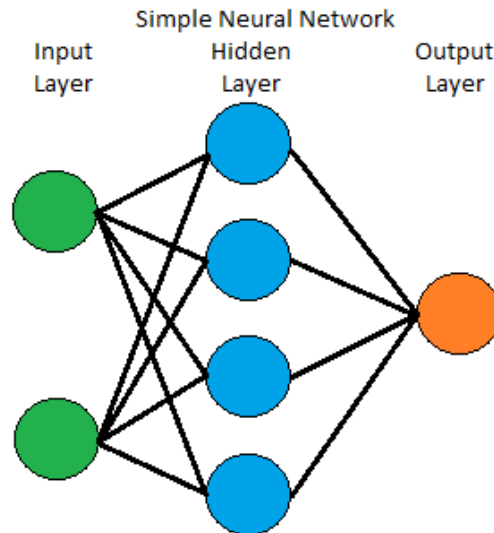


Figure 13: Simple Neural Network

### 2.4.1 Nomenclature

Many of the words that define the architecture of an artificial neural network come from biologically and neurologically inspired definitions. These definitions are been briefly explained in this section:

*Node / Neuron:* A node is represented by a circle as shown in Figure 13 above. It typically has a value between 0 and 1 and at the input layer it represents a feature that is desired to be found in data set. The nodes are also referred to as neurons.

*Synapses:* The biological name that connects two neurons together from the axon to dentrite. In Figure 13 above, the synapses are represented as the connecting lines between the nodes.

*Architecture:* Describes the formation of the neural network. It states the number of input layer nodes, followed by the number of hidden layer nodes, followed by the number of output layer nodes. The above figure is therefore described as having architecture of; 2-4-1.

*Input Layer:* The input layer is where the extracted features from a data set are entered into the network. The values entered at this layer are typically normalized from 0 to 1 and are calculated by overlooking the entire dataset. There are generally always more input nodes than output nodes, and generally at least two input values. There can be an infinite number of input nodes, but simply having more nodes may not actually be beneficial. Graphically speaking, the nodes are incrementally numbered from the top down.

*Hidden Layer:* The hidden layer is essentially where pattern recognition occurs. A standard neural network features a connection from each input to every single hidden node as well as a connection from every single hidden node to each output layer node. For the above 2-4-1 architecture there would be 12 synapses (4 synapses each from input layer nodes one and two, as well as 1 synapse connecting each hidden layer node to the output layer node). There can theoretically be an infinite number of hidden layers, however there is limited evidence to support that a large number of hidden layers are more beneficial than just 1 to 3 hidden layers.

*Output Layer:* The output layer is where the network returns the classification result. The number of outputs is equal to the number of features your network was designed to classify. The values presented in the nodes should be between 0 and 1 and thus each nodal result represents a degree of how much of that feature the network calculated.

*Weights:* Each synapse has a special quality describing the relationship between the nodes on each layer which are called weights. The weights are a representation of how much the node

from the previous layer influences the resulting output on the next layer. It is a multiple of the value present in the nodes, and is also typically between 0 and 1. It is important for all numbers to be normalized between 0 and 1 because of how many times values are multiplied together.

*Epoch:* Neural networks require to be trained by a set of training data. An epoch is a full iteration of all the training data one time through, and it is not uncommon for networks to take hundreds, or thousands of epochs before the network is considered ‘trained’.

*Learning Rate:* The learning rate is a feature describing how adaptive and how much information the network is willing to retain from a previous epoch. This value is between 0 and 1. A low value such as 0.1 will result in the network learning very slowly, but is also likely to be more accurate over time. A low learning rate does however result in a chance that a trained network state could be stuck in a local minima or maxima causing the network to be incapable of reaching its full potential.

### **2.4.2 Network Creation**

The ultimate goal for neural network classification is to minimize the predication error by finding an appropriate input-output relationship. This can be accomplished in many ways by carefully selecting the optimal factors describing the network such as the number of inputs, number of outputs, quantity of hidden layers and sample data, the training method (supervised or unsupervised), and the purpose of the network (classification or prediction) [26]. To understand the architecture and how an artificial neural network works, the following procedure outlines the calculations required to complete the first epoch:

### *Step 1: Determine Network Architecture*

The architecture of a neural network can have a significant impact on the final result of a chosen system and it is not obvious which architecture will be the best for a unique problem. A starting point is determining how many features will be describing the dataset. For example, let the number of inputs be 3 ( $I = 3$ ). Secondly, the number of output features should be able to be predetermined. Let the number of outputs be 1 ( $O = 1$ ). The final value to determine is how many hidden nodes to use in the middle layer. This value will typically be larger than the number of output nodes, and no more than twice the number of input nodes. Minimizing the number of hidden nodes reduces the amount of free variables [27]. For this example, let the number of hidden layer nodes be 4 ( $M = 4$ ). Therefore the architecture would be 3-4-1. It is important to note that it is improbable that this is actually the optimal architecture as there are many other ways that the network could be developed which may produce better results. It may eventually be determined that one of the input features may not actually have any effect on the output or even worse that it reduces the accuracy of the final output. If desirable, the architect of the network could run numerous simulations with different architectures to determine which inputs were ideal for the dataset.

### *Step 2: Initialize Values*

Synapses connecting each node need to have a starting weight value. This value is between 0 and 1 and can either be random or assigned a value from a set of previously saved weights. If this is a new architecture and dataset, then random values would be applied [24]. For this network, there would be 4 weights from each of the nodes in the input layer which influence the nodes in the hidden layer and 1 weight leaving each hidden layer node going to the output

layer. The weights from the input layer to the middle hidden layer can be denoted  $I\_to\_M\_weight[1\ to\ 3][1\ to\ 4]$ . In some neural networks, there is a constant threshold value associated with each node as well which is added on. These values can be randomized as well. The final initialization step is to normalize all of the input and expected output values. Datasets are typically large, and for increasingly larger datasets the network can be more effectively trained. To avoid unconstrained values, the entire dataset should be evaluated at the beginning during initialization, and normalized. If only the training data set is acquired, then there is a chance that the testing dataset could fall outside of the constrained values of 0 and 1 when normalized.

*Step 3: Calculate Middle Hidden Layer*

Calculate the value in each node in the middle hidden layer by summing up the input values multiplied by their weights (from the synapses) and adding a node threshold value (T) as shown in the equation below.

$$M[i] = \left( \sum_1^n I[n] * I\_to\_M\_weight[i] \right) + M[i] + T$$

This calculated value  $M[i]$  is then adjusted with a sigmoid logistic function below. This function allows the system to saturate large values where the limits of this output are 0 and 1 [28].

$$M[i] = \frac{1}{1 + e^{-M[i]}}$$

#### *Step 4: Calculate Output Layer*

After the hidden layer nodes have been calculated, the output layer can be calculated using the constrained values. A similar calculation is performed (compared to Step 3) but the inputs to this step are now the middle layer node values, and the resulting outputs are the nodes in the output layer. The updated equation is presented below:

$$O[i] = \left( \sum_1^n M[n] * M\_to\_O\_weight[i] \right) + O[i] + T$$

Once again this value is adjusted with the sigmoid logistic function to properly constrain the node to stay between 0 and 1.

$$O[i] = \frac{1}{1 + e^{-O[i]}}$$

#### *Step 5: Calculate Error*

When training the network, the correct output is known for all of the training data. The values found in the output nodes represent the theoretical classification calculated from the network. During early epochs, a correct value is not expected to be presented due to the inherent randomness created during the initialization step. The output error is found by subtracting the actual correct value from the calculated value at the output nodes and taking the absolute value:

$$error[i] = absolute(actual[i] - O[i])$$



### *Step 6: Update Hidden Layer Error and Weights*

The weights in the hidden layer can be adjusted in an attempt to minimize the output error. This is accomplished by traversing back through the network with the error calculated at the output layer. The hidden layer weight values are adjusted slightly by adding the product of the error at the output and the middle to output weight [25]:

$$M\_weight [i] = \sum_1^n M\_weight[i] + (error[n] * M\_toO\_weight[i, n])$$

This middle weight is used to calculate the error at the middle hidden layer. The middle node error is used to recalculate the input to middle weights:

$$M\_error[i] = M[i] * (1 - M[i]) * M\_weight[i]$$

### *Step 7: Adjust the weights between the middle and output layers*

A learning rate is commonly used to evaluate the degree of how much the network should update for each epoch. It is also a reference to the amount of the error that is removed. The value is set between 0 and 1, where higher values result in quicker learning rates but also tends to result in the algorithm oscillating the output accuracy. This oscillation can result in weak performance and classification [27]. Another common calculation includes using a momentum rate which is a factor of how much the result should change from previous epochs. It is essentially a memory of the previous epochs and normally a value between 0.5 and 0.9 [27]. The learning rate is applied with the follow equation:

$$M\_to\_O\_weight[a, b] = M\_to\_O\_weight [a, b] + (learning\ rate * M[a] * error[b])$$

The momentum is applied with the follow equation:

$$M\_to\_O\_weight[a, b] \\ = M\_to\_O\_weight[a, b] + (momentum\ rate * last\ M\_to\_O\_weight[a, b])$$

*Step 8: Adjust the weights between the input and middle layers*

The first layer also needs to be updated to reflect the changes that occurred in the later sections of the network. The weights between the input layer and middle layer are updated based off the error in the middle layer:

$$I\_to\_M\_weight[a, b] = I\_to\_M\_weight[a, b] + (learning\ rate * I[a] * M\_error[b])$$

Where 'a' is a number from 1 to the number of inputs and 'b' is a number from 1 to the number of hidden nodes. The final values that need to be updated are the threshold constants found at the middle and output layer nodes. They are updated exclusively from the error found in each layer and the learning rate:

$$M\_thresshold [ i] = M\_thresshold [ i] + (learning\ rate * M\_error[i])$$

$$O\_threshold [i] = M\_threshold [i] + (learning\ rate * error[i])$$

*Step 9: Check if training is complete*

These calculations have resulted in 1 epoch (out of hundreds or thousands) to have been completed, and the system needs to determine if more training is required. Training a network can take a long time, and it is up to the designer to determine when there is an acceptably low error. Typically networks will complete training when 1 of 3 conditions is met:

- 1) The system has trained up to a maximum number of epochs
- 2) The average error at the output has been minimized to an acceptably low value
- 3) The maximum error at the output has been minimized to an acceptably low value.

Ideally the 2<sup>nd</sup> or 3<sup>rd</sup> condition is met before condition 1, and condition 1 is usually encoded as a failsafe condition such that the network does not try to train forever. If the system has not met any of the conditions then another epoch needs to be run with all of the values updated again such that the error at the output is hopefully reduced.

#### *Step 10: Test the system*

Once one of the three conditions has been met, training is considered to be complete. All of the weights and threshold values have reached their acceptable values. A final set of testing data is then entered into the network and the output values will demonstrate the effectiveness of the system. The weights are not adjusted at this point, and the network is simply a one way architecture.

#### *Step 11: Remodel the Network*

If the output from the testing data is not considered acceptable then the network may need some changes. The maximum acceptable error and the average training error may need to be reduced or the number of epochs may need to be increased. If these parameters do not improve results, fundamental changes may need to be investigated. The learning and momentum rates can also be adjusted. Lastly, if none of the previously mentioned variable changes improve results, then a new architecture should be considered. Adding or removing a hidden layer node can have dramatic effects on how well a neural network can perform.

### **2.4.3 Notes**

It is important to note that running the same architecture multiple times will not necessarily produce the same results. This is due to the fact that random variables are created at the beginning. In order to reproduce the same results upon presentation, then all of the weights and threshold values are required to be saved. The network will then need to load these values in the initialization step instead of using random values. All of the same parameters describing the network will also need to be saved, which include the learning rate, momentum rate, architecture, and order of features from the input data.

### **2.5 Summary**

Electronic noses share a lot of similarities with their biological counterpart. Both e-nose's and the human nose will use complex pattern recognition techniques and identifiers to label airborne compounds which are used for analysis by a computation unit. The sensors selected for the electronic noses typically are chosen to target specific chemicals and in this thesis, FiS and Figaro sensors were chosen to withstand high concentrations of ethanol. The mathematical intensive neural network approach has been outlined and it has been accepted that it is a successful method to discover complex patterns.

## Chapter 3

### 3 Literature Survey

This chapter investigates the previous research that others have performed into the development of electronic noses and specifically how they have been applied in the alcohol industry. Secondly, it outlines the most popular analysis methods regarding the data extracted from the electronic nose sensors.

It is important to investigate multiple methodologies to analyze the data acquired because electronic noses generate multi dimensional data which is difficult to visualize and interpret [29]. Gas mixtures are very complex and not typically a straight forward relationship of adding two known gases together. Unknown components found in low concentrations can also dramatically shift the response from the sensors. The gas sensor response is usually non-linear when used against a ramped concentration of known gas which adds to the complexity of the problem [30]. To solve these issues, there have been multiple models applied and some have shown more success than others.

#### 3.1 Known Uses of Electronic Noses

Electronic noses are becoming more popular with the large improvements to the computer world. These devices have successfully been able to sense compounds and have been used for quality analysis for wine, cola, meat, fish, tea, and coffee [31]. Siripatrawan et al have been able to detect diseases such as Salmonella Typhimurium[29]. These devices are being considered as a suitable replacement for human judgment of products and there exists a co-relation of sensor data compared to the tester's analysis [31]. The threshold point of sensing a smell for humans is considered to be the point where only 50% of the people can detect the odor [32]. Given that half

of the population cannot detect specific airborne chemicals at known concentrations, a high demand for some electronic nose chemical sensors could exist.

### **3.2 Data Feature Extraction Methods**

The data collected from an electronic nose is considered to be a collaborative digital fingerprint of all of the gases found inside the chamber. Recreating trial results is accomplished by observing the same pattern output across numerous sensors and thus an operator needs to recognize the 'blueprint' for each sample. Discriminate Factor Analysis (DFA) and ANN are considered to be a few of the more popular advanced pattern recognition techniques. These methods offer complementary information which together will reinforce an analysis verdict [29].

Analyzing salmonella, Siripatrawan et al were able to use a 12 input, a 10 node hidden layer, and 1 output layer ANN to obtain a  $R^2$  value equal to 0.998. They used a hyperbolic tangential sigmoid function in the network for normalizing values. Multivariate analysis can be used to withdraw features that can be used as inputs into the network [29]. These networks have advantages over other techniques which can allow for adaptability to new odors, as well as have a noise and fault tolerance [32].

Figure 14 below shows the architecture of the network that was used to successfully identify five alcoholic odors from an electronic nose that used twelve tin-oxide sensors. A similar example used a back propagating neural network with multi-layer perceptron (MLP) to analyze culture growth of bacteria which achieved a 96% classification success rate (360 training elements, and 360 test elements) [25]. Three layer neural networks are popular because they can solve any classification problem [25], are logical once it is trained, and the analysis is quick to trial [32].

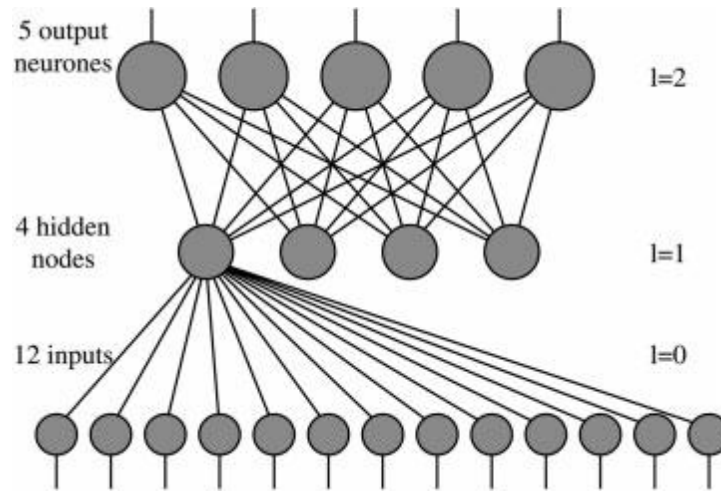


Figure 14: Structure of fully connected three-layer back propagation network [25]

Various steps of hidden nodes have been tested in the past to determine what the best configuration was for a data set. To evaluate a brain to signal interface, N. Huan et al varied the number of hidden nodes from 20 to 100 in steps of 20 to determine the best configuration [33]. This experiment was also tested using LDA and MLP-BP NN, and it was determined that data segmentation should be avoided because upon testing, it compared negatively to a full signal analysis. It also increased the computational complexity and increased the time for training and testing [33]. This approach with LDA and MLP-BP was able to achieve a 97.00% classification success rate. There are more advanced neural networks which could be considered. Y.H Tay et al showed that a Fuzzy ARTMAP neural network outperforms the common back-propagation based multi-layer perceptron for advanced pattern recognition [34].

Principle Component Analysis (PCA) and Linear Discriminant Analysis (LDA) are also popular methods to classify an odor. PCA was used to detect the quality of black tea, a product where over 500 chemicals are found (both volatile and non-volatile). The cluster display for the PCA was able to graphically distinguish 10 different qualities found in the tea samples. The approach

by Kashwan and Bhuyan also found that an increase of 4% to 5% was found in the performance when sensor drift compensation was added [31].

Apart from sensor drift compensation, baseline adjustments can improve the results of a classification. To create consistent comparable data, the response can be adjusted to become relative to the baseline of the sensing chamber. This is often calculated by finding the maximum change in the sensors response divided by that of the initial resistance [29].

$$\text{Relative resistance} = \frac{\text{Resistance}_{max} - \text{Resistance}_{min}}{\text{Resistance}_{baseline}}$$

### **3.3 Hardware implementation**

Some of the first electronic noses were tested and created in 1980 by using an array of gas sensors with pattern known pattern recognition techniques [32]. Today there exists commercially available portable electronic noses such as the Cyranose 320, Airsense PEN2, and Airsense PEN3. The Applied Sensor Company alone has sold more than 100,000 units of their Air Quality Module which is used to detect VOCs and other odors in living spaces [20].

Arguably one of the most important components of the electronic-nose apparatus is the gas delivery system to the sensors (in conjunction with the sensing apparatus). One of the simplest methods is by analyzing the headspace of a sample. The headspace can accumulate overtime by being kept in a sealed compartment and released into the sensing chamber. Improvements to this system include a clean air delivery system to the chamber (such as CO<sub>2</sub> or N<sub>2</sub>), or needle injection to the target sensing region [20]. Rigorous standards can be applied to this delivery system where the temperature of the injection syringe is even controlled before the collection of



headspace gas [29]. Adhering to systematic routine will improve the performance and reliability of collected results.

Between samples, most if not all electronic nose chambers need to be cleaned such that the next test is referenced against the same baseline as the previous samples. Cleaning the chamber can be achieved by using a known baseline reference gas or by using fresh air from the outside environment. Previous experiments have various ranges for the time required to clean the chamber. R Chutia and M Bhuyan required 30 minutes of fresh air before taking a new sample [21].

Inside the sensing chamber, the sensor array is found. Most sensors such as the TGS, and Figaro gas sensors require that they be heated and thus will increase the temperature of the chamber. Humidity and temperature control are typically added to maintain a stable environment [20]. Taguchi gas sensors require approximately 1W of power to operate and the sensing element can reach temperatures of 350°C. This high temperature is common for all metal oxide sensors for them to operate properly [32]. Most sensors inherit the hazard of drifting results over time. This drift in sensor response can however been compensated for by using an approximate analysis, linearity assumptions, or ANN's [35].

### **3.4 Summary**

The studies presented in this chapter have shown that artificial neural networks have been successfully applied and are regularly used in the food and beverage industry as a method for classification. They regularly achieve a successful classification rate above 90%. The considerations and recommendations found from published papers has helped with the design and creation of the electronic nose prototype by optimizing the gas delivery system and by

offering known methods to clear the chamber between samples. Although a majority of the known uses have not been applied to the analysis of heavy spirits such as whisky, many successfully attempts with wine, cola, meat, fish, tea, and coffee offer important guidance.

## Chapter 4

### 4 E-Nose Box Design

The electronic nose used for this project was to be a new design and started from scratch. All of the parts in the final prototype were custom designed or independently selected to help analyze the chemicals from Pernod-Ricard and to evaluate common alcohols. This chapter covers the development process and justifies the design choices. An overview of the final prototype is shown below in Figure 15 with the major component part list following in Table 8.

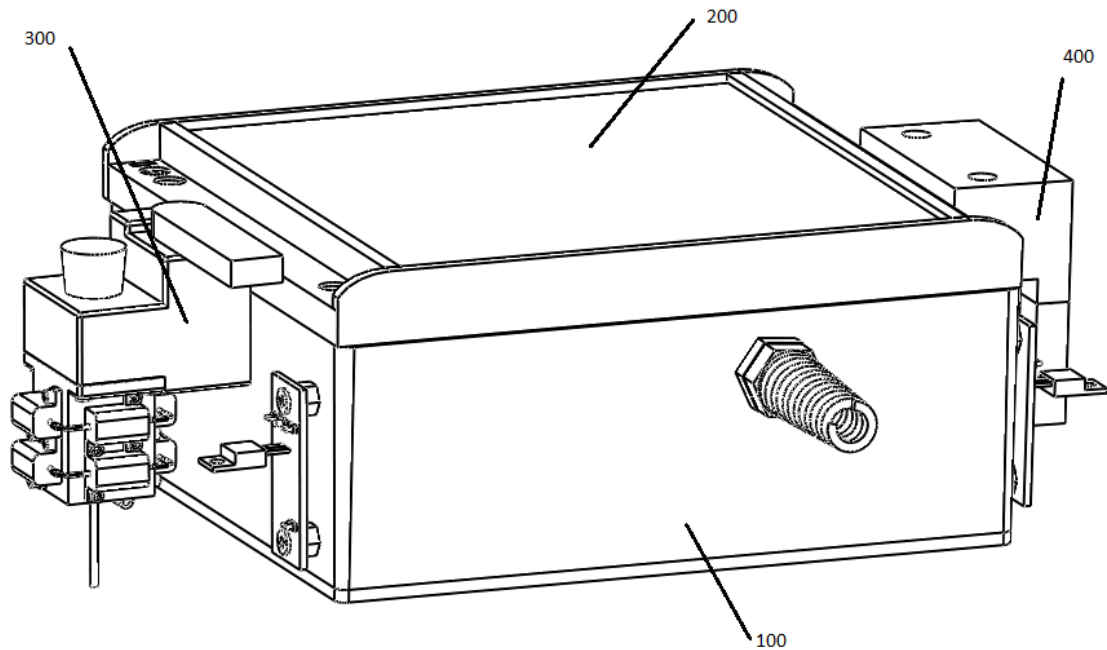


Figure 15: Electronic Nose Final Prototype

<b>Final Prototype Major Component List</b>	
<b>Part Number</b>	<b>Name</b>
<i>100</i>	Hammond Chamber
<i>200</i>	Hammond Chamber Top
<i>300</i>	Heating Block
<i>400</i>	Motor Fan Block

**Table 8: Final Prototype Major Component List**

#### **4.1 Dimensions**

A chamber to monitor and contain the samples was necessary to perform the experiments. This housing needed to meet many qualifications for the project. For consistency, it was not to be prone to contamination. It had to be able to be cleaned and aired out without much difficulty because a large number of samples would be trialed inside of the chamber. Understanding that the future direction of the electronic nose was to be a portable handheld device, size was taken into consideration and a small construct was chosen. This would allow for easier stepping stones when reducing the size in the future.

To mimic a portable design, all of the electronics and components required for data collection were to be included inside of a contained unit. In addition to the sample gas inside the box, the electronics posed as a possible contamination issue, but modifications to the design could be re-evaluated in the future to minimize contact. Aluminum is a popular metal to work with and there exist many commercially available aluminum products able to be used as an enclosure. Aluminum will suffer from contact with liquid Ethanol but only has limited contamination to the gas from the Ethanol spirits that would flow into the chamber. An aluminum structure would decrease the development time due to the availability of products and could be used as a prototype.

Hammond Manufacturing offered an array of modern, high quality instrument enclosures. The top cover and main enclosure are both made out of die cast aluminum (G Al Si 12 / DIN 1725). This product was also available for purchase with a standard powder coating, but this option was rejected to reduce the amount of possible contamination. The final piece in this product is a standard thermoplastic gasket which settles between the lid and box to make the chamber water tight. The gaskets are rated from -40°C up to 120°C. The three pieces are held together by 4 captive stainless steel screws. The chamber required at least four openings to allow for samples to be administered which were:

- 1) Sample Chamber Inlet opening
- 2) Mixing Fan opening
- 3) Clean air inlet
- 4) Contaminated air outlet.

Inside the chamber, it was necessary to be able to house a mixing fan, a TWR-K40X256 data logger and PCB to house the replaceable sensors. Given the stage of the project, the box was selected prior to completion of the PCB, but it was desirable to be able to fit 8 to 20 sensors inside of the chamber. The PCB was then later fabricated to fit inside with the fixed dimensions of the chamber.

The known dimensions to be placed inside the chamber were only that of the Freescale TWR-K40X256 microcontroller board, and the fan blade. The fan blade itself was 18.25 mm wide and 37mm high which would take up a total volume of 19.62cm cubed while spinning. The TWR-K40X256 board was powered by a Freescale Kinetis K40 CPU and held dimensions of 105mm (length) by 90mm (wide) by 15mm (high).

Hammond offered box sizes from; width of 50mm up to 200mm, length of 75mm up to 330mm, and depth (including lid) from 33mm up to 120mm. This meant the available volumes were between 123.750cm cubed, and 7920cm cubed.

The variety of sensors that were purchased initially operated under peak conditions when 1L of air was available per sensor. It was understood that despite being able to accommodate between 8 and 20 sensors in the box at a time, only a limited quantity of them would be used at any given time through selective reasoning after analyzing samples.

The Hammond Box selected was the Hammond R191-170-000 and was sized as follows:

- Width: 170mm
- Length: 200mm
- Depth including Lid: 90 mm
- Volume: 3060cm cubed.

This volume allowed for approximately 2.5L of air inside the box once all other components were to be assembled inside.

## **4.2 Heater Design**

The electronic nose design required a convenient way to be able to interchange samples between experiments. To standardize each sample, a heating chamber was required to ensure consistent results. Lab conditions were expected to change because the demonstration location would change from time to time, thus a heater would help to minimize the changes from the environment and be beneficial for analysis. The boiling point of ethanol is 78.1°C, which determined the minimum temperature requirement for a heating chamber in case a field tester wanted to evaporate the sample. Water was also a large component to each sample since

premade samples were diluted down to 20% ABV with water. Creating a heating chamber to operate at 100°C would also be useful benchmark in the event the operator wanted to evaporate the water.

Multiple models for a heater were investigated and designed such that the primary objective was met to ensure consistency between samples and for ease of use. The heating chamber was ideally placed outside of the chamber to minimize the amount of heat generated inside. The primary sensors purchased (Figaro SB15, Figaro TGS 2610C and TGS2610D) reported that peak operating conditions were at 40% relative humidity in the air. Increasing the temperature inside the box would result in a lower level of relative humidity. A custom design heater would allow for these constraints and criteria to be met compared to store bought heater which may lack a desired quality.

Methods investigated for purchase included ‘heat pads’; such that a drop of a sample could be placed and heated up until completely evaporated. This method had many problematic areas though; it would need to be cleaned each time and would most likely be placed inside of the chamber which would be irritating to access between samples. To minimize the amount of the times that the operator would need to open the chamber meant that the heating unit needed be placed outside the primary sensing chamber. A temperature controlled, valve operated unit was considered to be the ideal design. An exploded view of the top half of the designed heater is presented below in Figure 16. The respective major components list for the top half of the heater block is listed in Table 9.

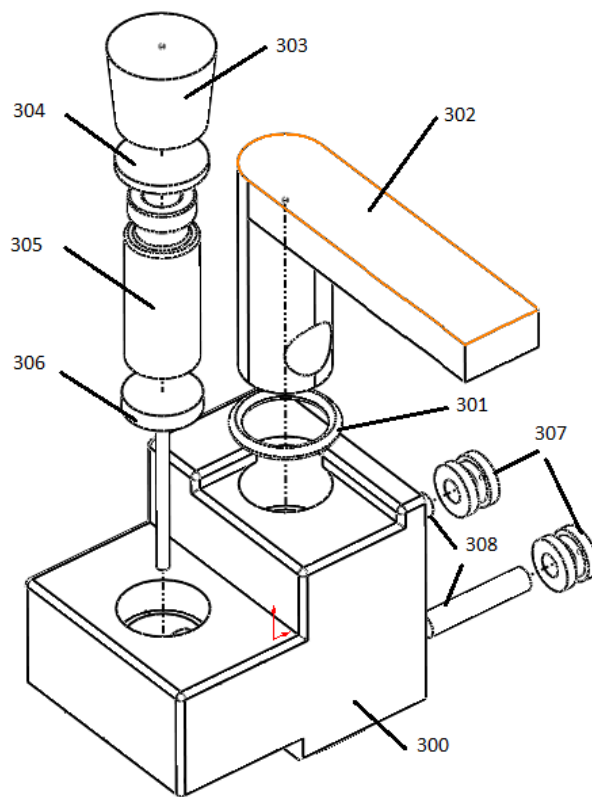


Figure 16: Vial Heater Top Section

Vial Heater Top Section Part List			
Part Number	Name	Quantity	Material
300	Vial Heater Top Section Block	1	Aluminum
301	O-Ring	1	Rubber
302	Valve	1	Aluminum
303	Rubber Stopper	1	Rubber
304	Septa	1	Rubber
305	Vial	1	Glass
306	Vial Lift Pin	1	Aluminum
307	Nut	2	Brass
308	Mounting Screw	2	Steel

Table 9: Vial Heater TopSection Part List



To minimize the amount of cleaning required between experiments, the samples were to be placed into 2mL glass disposable target vials that would fit inside an enclosed heating area. Conventional gas chromatography methods use less than 5  $\mu$ L per sample and so a 2mL disposable vial would be more than enough to house a liquid or solid sample and be large enough to easily handle. The disposable glass vials would also allow solids to be placed inside and measured as well if desired. These vials were 32mm tall, with a base diameter of 12mm.

To be able to easily change samples, a push pin would be used inside the base of the heating block. This pin would be just large enough to have a vial rest on it but would allow the operator to easily lift the vial out of the enclosure. A rubber cork was used to seal in the sample and disposable septa were used between the cork and sample to minimize contamination.

The larger top section of the heating block was to contain the cork, septa, valve and connection mount to the actual Hammond box chamber. A custom valve was designed that was integrated into the heating block. The 1.5 mm septas were selected because they were the largest, most inexpensive septas available and had a larger diameter than the vials diameter. These septas were exclusively used to minimize contamination from a size 8 (16mm base) rubber stopper which is primarily used for larger chemical flasks.

The size of the valve was also designed to be as small as possible given the other determined dimensions. The height needed to be higher than that of the stopper, and it needed to be long enough to open and close the access to the hollowed out flow path for the samples. A gasket was also placed around this valve to minimize the amount of sample that escaped the heating block.

The bottom half of the heater and it's respective parts are listed below in Figure 17 and Table 10.

Vial Heater Bottom Section Part List			
Part Number	Name	Quantity	Material
350	Vial Heater Bottom Section Block	1	Aluminum
351	Heat Conductive Tape	1	Tape
352	Temperature Sensor	1	N/A
353	Temperature Sensor Screw	1	Steel
354	Heat Block Connection Screws	4	Steel
355	Resistor	8	N/A
356	Resistor Screw	16	Steel

Table 10: Vial Heater Bottom Section Part List

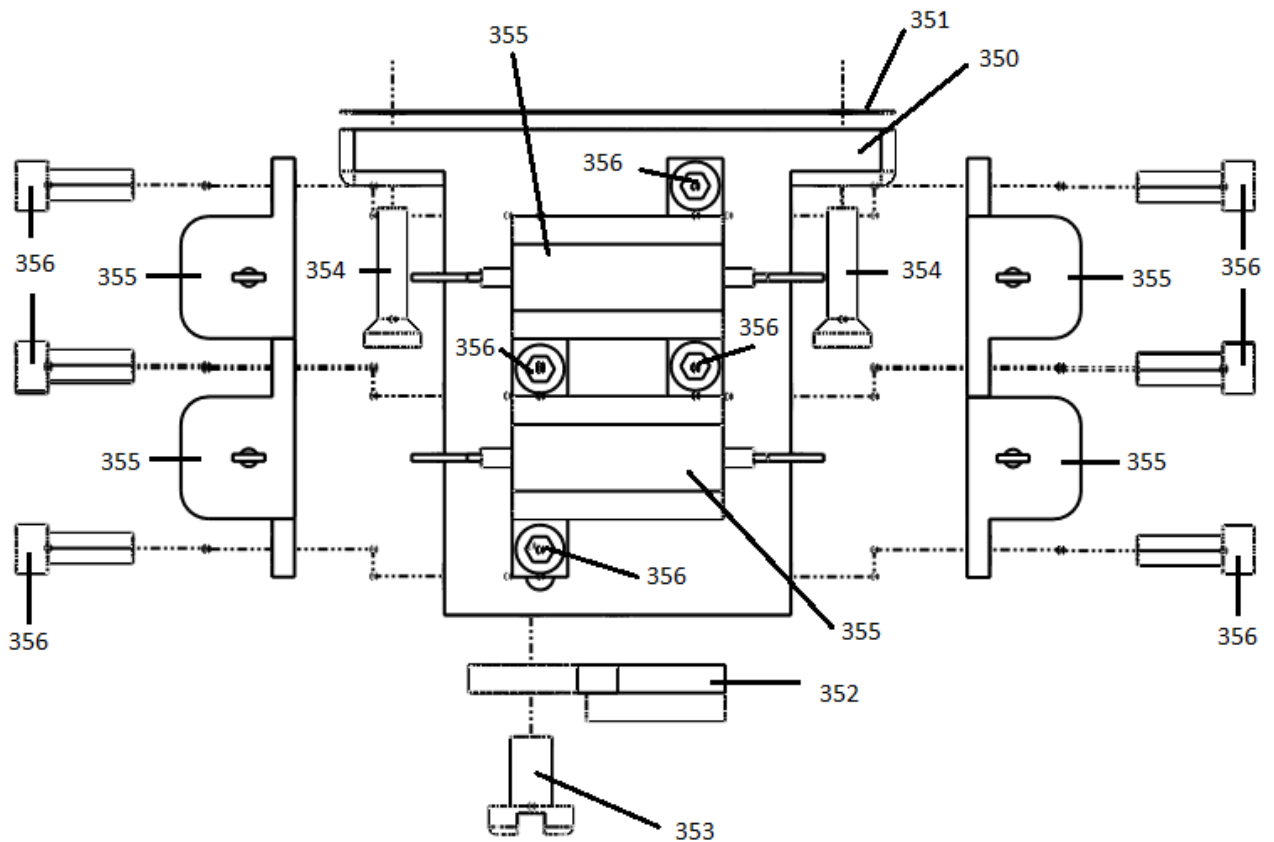


Figure 17: Vial Heater - Bottom Section

Resistors were to be used to directly heat up the sample chamber. With power being limited, this meant that the heating block was required to be made with a high heat conducting material and use a minimal amount of material so it would heat up faster. A low ohm resistor that could handle high power was selected to transfer the heat it generated to the block. A flat sided 0.5Ω 5W resistor was selected. The flat side measured 15.20mm, by 8.82mm with two adhering pads to be used to mount the resistors with screws and thermo conducting paste.

The large block was to be mounted to the Hammond box main chamber by 2 threaded pins, and nuts would be fastened on the inside to secure the heater in place. Apart from the two pin holes, the sample inlet hole would also need to be drilled into the box. To minimize the amount of heat transfer to the aluminum box, more layers of heat resistive tape were adhered between the heater chamber and Hammond Box.

The size of the resistors and vials were the limiting factors to the minimal size of the heater block. The final design would be just large enough to contain these instruments and the push pin. The base block being heated was 25mm by 25mm and had a height of 40mm. To limit the heat transfer to the valve section of the heater block, heat resistive tape was used in multiple layers to minimize heat transfer from the base block to the top large block. This base block was securely held in place by 4 screws.

The resistors were coated with thermal paste to improve heat transfer to the metal and then secured onto the block with screws. A total of eight resistors would be able to fit onto this small section. A power supply to offer 2.5A would be required to operate the resistors, so the resistors were connected in series and parallel to use all the available power. The final component added

to this heating block was a temperature sensor which was placed on the very bottom. This location was closest to where the liquid sample would be placed.

The final version of the heater shown below in Figure 18 was very similar to the initial designs with the exception that heating tape was used in areas that were prone to being touched which would minimize the amount of contact between the user and the hot surface. The left half of the image is the top view of the heater, and the right side shows the side view of the heater.

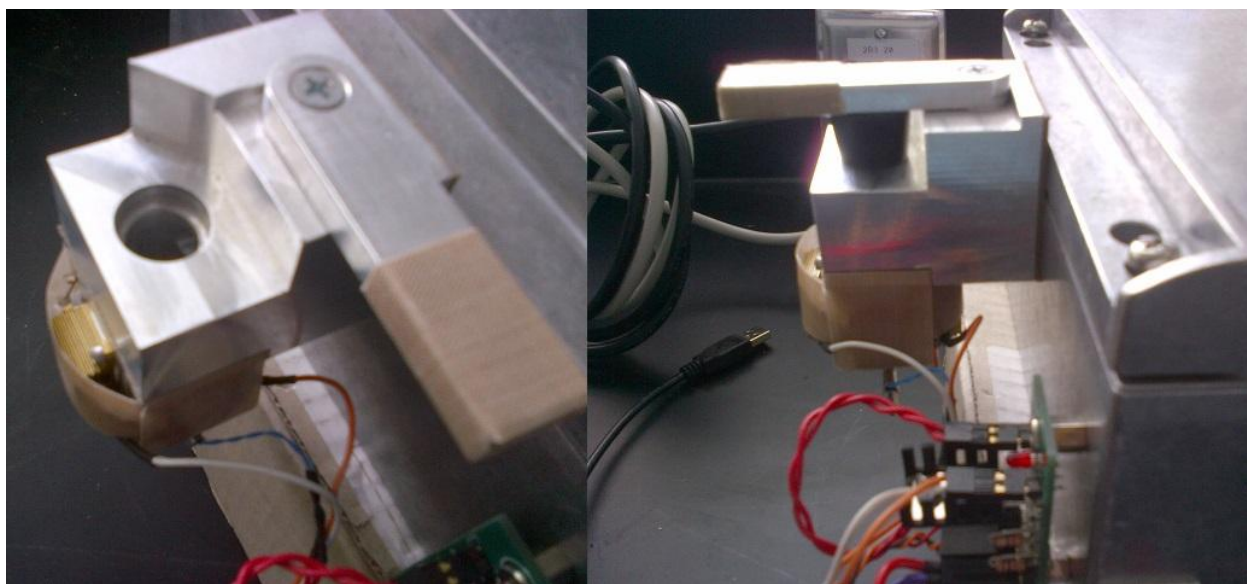


**Figure 18: Vial Heater System Final Prototype**

The heater was able to output approximately 90°C on the maximum setting. This temperature was ideal for being able to control the state of Ethanol. The design of the heater made the entire block become hot and thermo tape was used in multiple areas to limit the amount of heat transfer. The 2D drawings for the fabricated heater are shown in Appendix A – 2D Drawings in Figure 40 and Figure 41.

### **4.3 Fan Mount Design**

To evenly distribute the air inside of the chamber, a mixing fan was deemed necessary to the overall design. To minimize the amount of heat generated inside the chamber, the motor for the fan was placed on the outside of the Hammond Box. The designed motor mount appears below in Figure 19: Motor Mount Exploded View. A brushless DC motor (Part Number: 402) that operated at varying speeds was used to spin the fan blade (404). It operated between 0 and 5V and required an extension pin (403) such that the fan blade would safely fit inside of the chamber.

Two aluminum motor mounts (401 and 402 in Figure 19) were created to securely hold the motor while the nuts (406) and bolts (407) firmly attached the structure to the Hammond Box. This design was selected so that the motor could be removed or replaced in the future. It also allowed for easy wiring connections to the power supply and control modules. The 2D drawings for the fabricated motor mount are shown in Appendix A – 2D Drawings in Figure 38 and Figure 39.

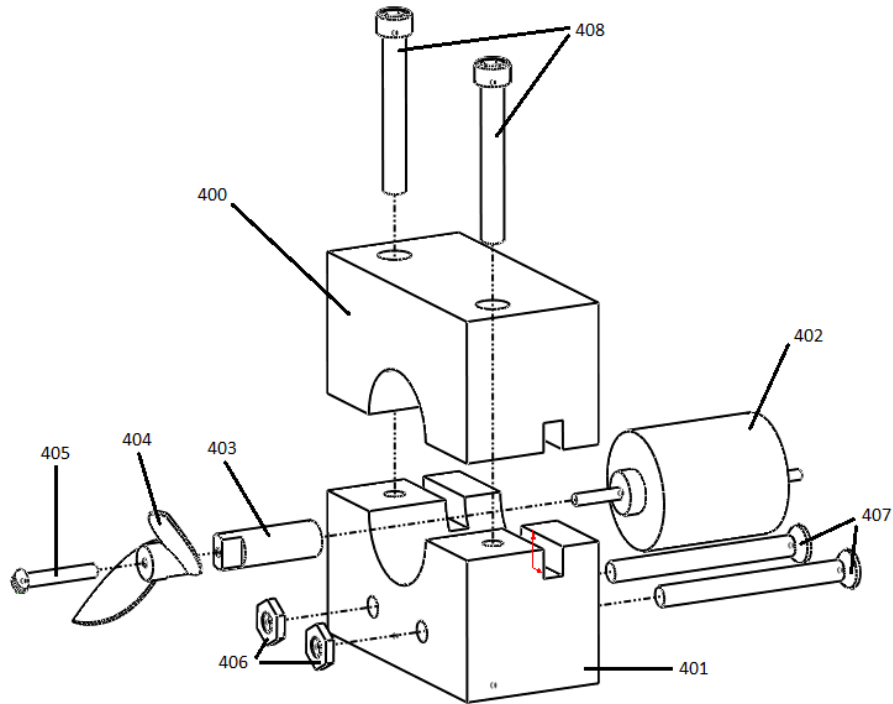


Figure 19: Motor Mount Exploded View

Table 11 below lists the parts found in Figure 19 and what material was preferred for the part.

<b>Motor Fan Mount Part List</b>			
<b>Part Number</b>	<b>Name</b>	<b>Quantity</b>	<b>Material</b>
400	Motor Top Support Block	1	Aluminum
401	Motor Bottom Support Block	1	Aluminum
402	Motor	1	N/A
403	Motor to Fan Connection Rod	1	Stainless Steel
404	Fan Blade	1	Brass
405	Fan Blade Screw	1	Steel
406	Fan Block Support Nut	2	Steel
407	Fan Block Support Screw	2	Steel
408	Fan Block Connection Screw	2	Steel

Table 11: Motor Fan Mount Part List

#### **4.4 Airline Filtration**

To standardize samples, the Hammond Box chamber needed to be cleaned out between trials. This required that the chamber be flushed out of the contaminated air and replaced with new clean air. To ensure that similar conditions were met a humidifier and pressure regulator were used. Air lines from a lab bench were used to provide an unlimited supply of air. This air flowed through an analog pressure regulator, then through NSF-51 certified clear PVC tubing and exited from a submerged air stone. The air stone selected was called the *Mist Air Stone* by *Marina* (A983). It was selected due to low cost, ease of replacing, and ease of installation. The air flowing out of the air stone would bond with the water as it rose through the 200 mL of water which increased the moisture level. This humidified air was then finally redirected into the Hammond Box chamber to flush out the box. The airline filtration system is shown in Figure 20 and Figure 21 below.



Figure 20: Airline Filtration System- Internal

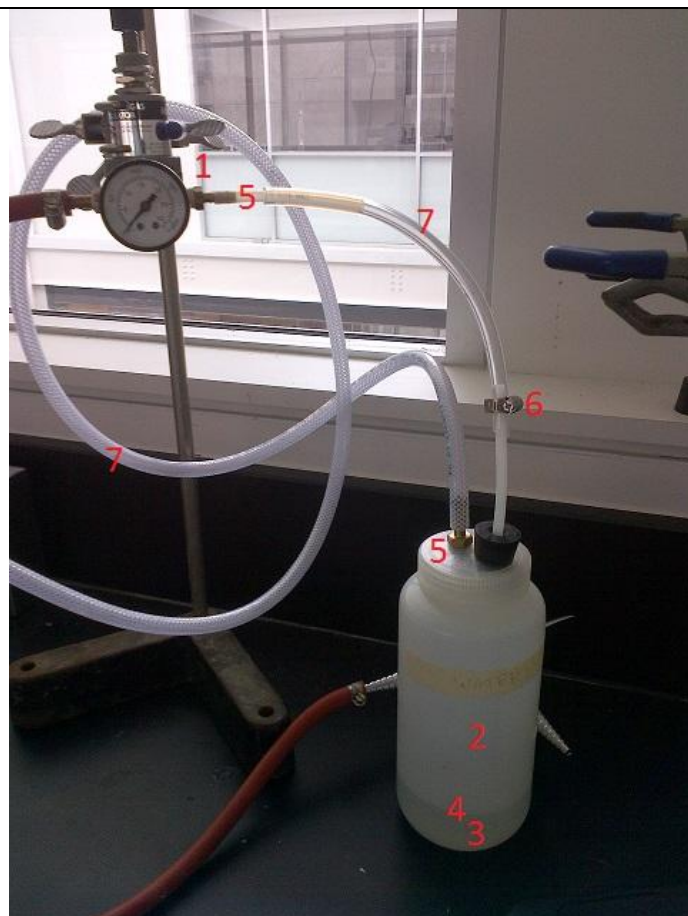


Figure 21: Airline Filtration System - All

The materials used are listed as follows: 1) Analog Pressure Regulator, 2) Graduated Cylinder , 3) Water, 4) Air Stone, 5) 0.75 Inch Barb Hose, 6) Sealing Brackets, 7) Three Tubes

#### 4.5 Summary of the Overall Design

The final design featured all of the above sections put together. The exploded view of all of these components with the exception of the air line filtration can be pictured below in Figure 22: Final Design Exploded.



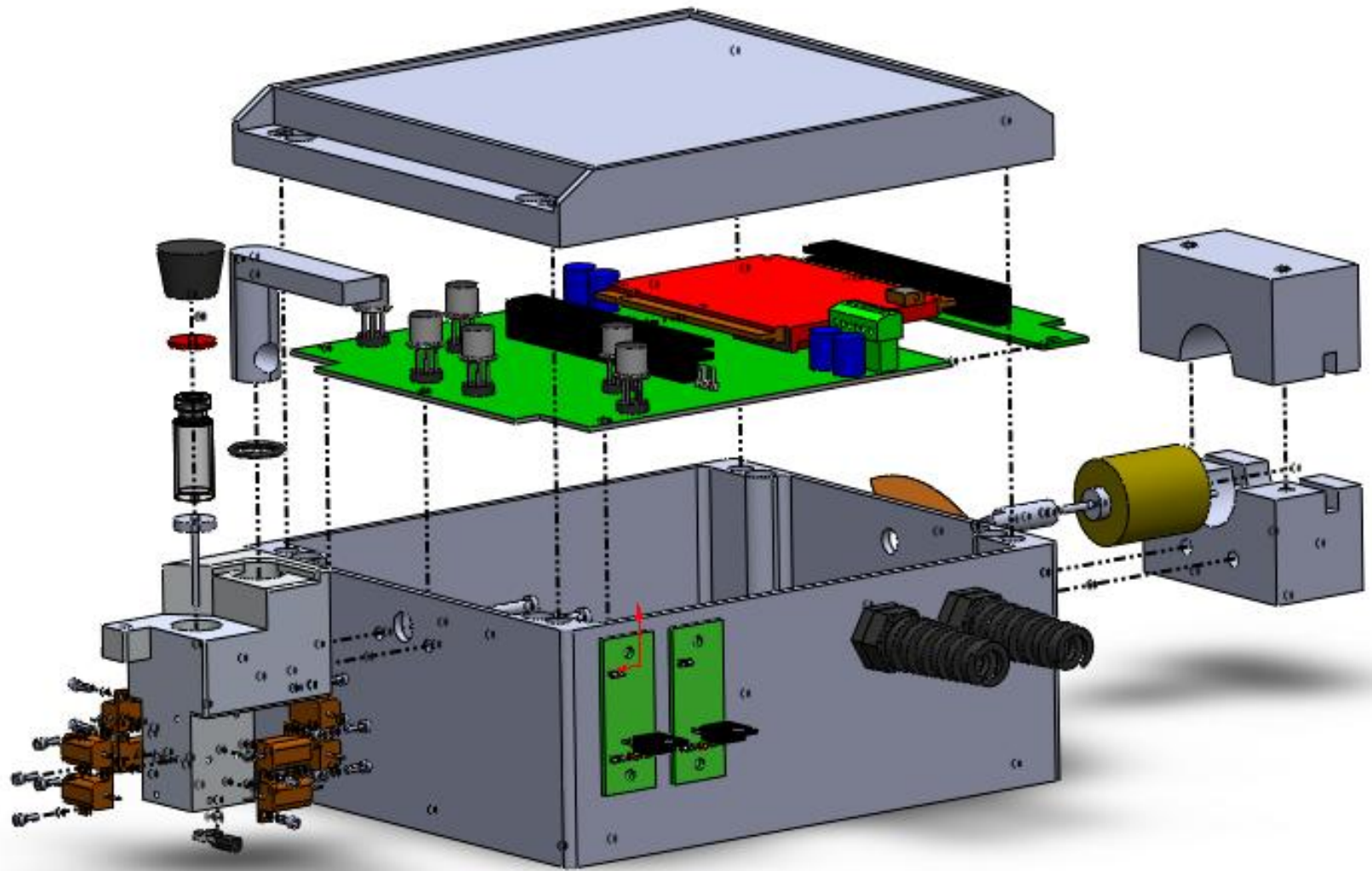
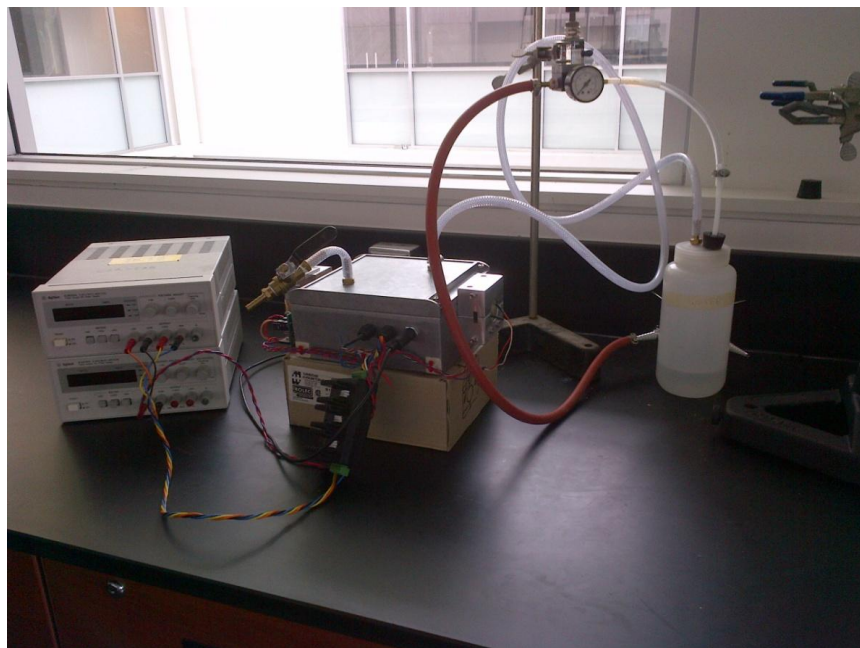


Figure 22: Final Design Exploded

The final hardware setup appears as shown in Figure 23 which features the power supplies, electronic nose, heating block, fan, air inlet and outlet, air humidifier and lab bench air inlet.



**Figure 23: Electronic Nose Setup**

The inside of the chamber is shown below in Figure 24.

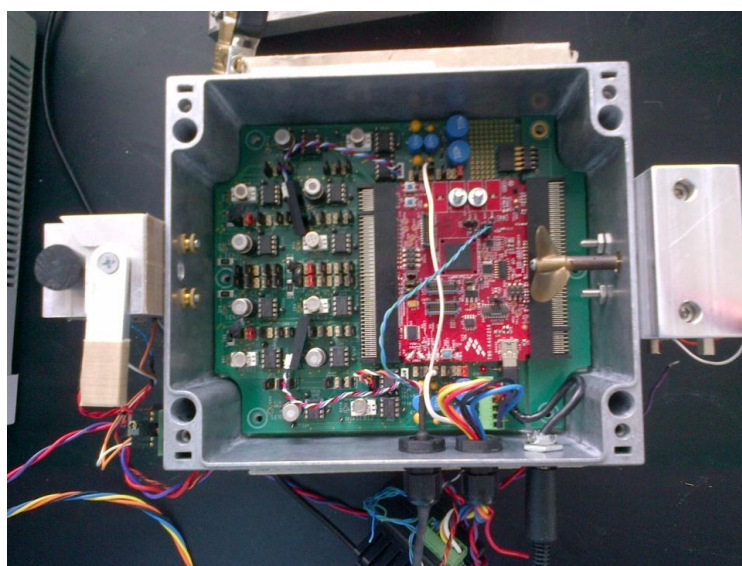


**Figure 24: Electronic Nose Internal Chamber**

## Chapter 5

### 5 Experimental Procedures and Trial Results

The prototype system that was created required rigorous testing to be able to provide valuable results. Any potential problems found, were fixed or modified to allow for a working lab bench electronic nose. Numerous systematic testing methods were trialed to test the limits on what the prototype was able to achieve. The setup procedure and testing process is presented in this chapter with their respective results.

#### 5.1 System Setup

Berry Punch was the name of the interface used by the electronic nose that displayed the real time output of the sensors from inside the chamber [36]. From an operator's perspective, it was primarily used to control the sample heating chamber temperature, fan speed, and sensor resistor values. It communicated with a Serial Relay program that handled the communication between the K40 board inside the chamber and the user interface [36]. The following screen shot (Figure 25) shows the available options that a user could control. The top twelve rows list the 12 sensors inside of the chamber that detected Ethanol and air quality. Turning off a multiplexor disabled a sensor, and in order for the sensor to properly operate, the heater for each sensor was required to be on. In this case, they were all set to a constant 5V. In the multiplexor column, the resistor values were set for each sensor, and each had four available options to choose from which determined the sensitivity.

Connected to Localhost:8000 - BerryPunch

File Capture

System Capture Processes

### Sensor Array

ID	Cell Type	Status	Multiplexer	Heater	Raw	V	$\Omega$
SEN1	TGS2610C	Enabled	Off 10 k $\Omega$	Off Line V = 0.00V	65535	3.30 V	5.152 k $\Omega$
SEN2	TGS2610C	Enabled	On 2.49 k $\Omega$	On Line V = 5.00V	22512	1.13 V	8.493 k $\Omega$
SEN3	TGS2610C	Enabled	On 10 k $\Omega$	On Line V = 5.00V	17606	0.89 V	46.399 k $\Omega$
SEN4	TGS2610C	Enabled	On 10 k $\Omega$	On Line V = 5.00V	27918	1.41 V	25.567 k $\Omega$
SEN5	TGS2610C	Enabled	On 2.49 k $\Omega$	On Line V = 5.00V	30187	1.52 V	5.7 k $\Omega$
SEN6	TGS2610C	Enabled	Off 10 k $\Omega$	Off Line V = 0.00V	65535	3.30 V	5.152 k $\Omega$
SEN7	SB-15-00	Enabled	Off 24.9 k $\Omega$	Off Line V = 0.00V	7460	0.38 V	2.023 k $\Omega$
SEN8	SB-15-00	Enabled	On 24.9 k $\Omega$	On Line V = 5.00V	19250	0.97 V	5.988 k $\Omega$
SEN9	SB-15-00	Enabled	On 24.9 k $\Omega$	On Line V = 5.00V	11926	0.60 V	3.399 k $\Omega$
SEN10	SB-15-00	Enabled	On 12 k $\Omega$	On Line V = 5.00V	25627	1.29 V	4.174 k $\Omega$
SEN11	SB-15-00	Enabled	On 24.9 k $\Omega$	On Line V = 5.00V	16251	0.82 V	4.873 k $\Omega$
SEN12	SB-15-00	Enabled	Off 24.9 k $\Omega$	Off Line V = 0.00V	7570	0.38 V	2.055 k $\Omega$

ID	Cell Type	Status	Raw	V	$^{\circ}\text{C}$
NTC1	HTG3535CH:	Enabled	14744	0.74 V	46.2 $^{\circ}\text{C}$
NTC2	HTG3535CH:	Enabled	14459	0.73 V	46.9 $^{\circ}\text{C}$
VIAL	B57703M103	Enabled	11729	0.59 V	60.0 $^{\circ}\text{C}$

ID	Cell Type	Status	Raw	V	%R.Hum
HUM1	HTG3535CH:	Enabled	33509	1.69 V	25.1 %RH
HUM2	HTG3535CH:	Enabled	38798	1.95 V	34.8 %RH

Connected to Localhost:8000 | Vial: 60.00 $^{\circ}\text{C}$  / 60.03 $^{\circ}\text{C}$  / -0.03 $^{\circ}\text{C}$  | Fan: 0 %

12:08 PM 2013-07-19

Figure 25: Berry Punch Operators Interface - Resistor Select

The resistors were in series with each sensor, so when the final resistance measurement inside the box was closest to the multiplexor resistor value that meant the output would be more accurate. This is because the sensor and the resistor each approximately drew an equal amount of the current. When setting up the environment for electronic nose, the following guidelines were used:

### **5.1.1 System Tab**

*The System tab controls the default characteristics inside of the Hammond Box.*

- 1) Start the Berry Punch software.
- 2) Plug in USB connection from Hammond Box to PC.
- 3) Run Serial Relay software.
- 4) In Berry Punch connect to the system: File - > Connect.
  - a. To connect to the software, the name needs to be “Local Host”, and IP set to 8000.
- 5) Wait for the multiplexor values to automatically turn on (approximately 10 seconds).
- 6) Turn on the heaters for sensors 2, 3, 4, 5, 8, 10, 11.
- 7) Adjust default multiplexor resistors:
  - a. Change sensor 2 from 10K  $\Omega$  to 2.49K  $\Omega$ .
  - b. Change sensor 5 from 10K  $\Omega$  to 2.49K  $\Omega$ .
  - c. Change sensor 10 from 24.9K  $\Omega$  to 12K  $\Omega$ .

### **5.1.2 Capture Tab**

The Capture tab showed the real time output from the sensors inside the chamber. The electronic nose used 7 of the 12 chemical sensors inside of the chamber for analysis. The 4

perimeter sensors (Sensor #s 1, 6, 7, and 12) were temperature modulated and were not used for this study. Sensor number 9 was a duplicate of an air quality sensor which was also not used for analysis.

- 1) Select the Capture tab (beside System tab).
- 2) Uncheck sensors 1, 6, 7, 9, 12 so that they are not graphed on the screen. The output from these sensors is not used in the final analysis.
- 3) Right click on the graph module and change the history, as well as the minimum and maximum scales to graph. The minimum value needs to be adjusted first.
  - a. Right Click -> Resistor -> Minimum -> 1000.
  - b. Right Click -> Resistor -> Maximum -> Automatic.
  - c. Right Click -> History -> Everything.
- 4) Clear the history so that the output does not show the times and disturbances for when the sensor resistors were being changed.
  - a. Click 'Capture' (beside File) -> Reset Capture.
- 5) Change Default timers in the bottom right corner.
  - a. Timer 1 set to 1:00.
  - b. Timer 2 set to 4:00.

### **5.1.3 Processes Tab**

The Processes tab controlled the vial heater temperature set point, as well as the PID control logic. The PID controller did not need to be adjusted because it had already been tuned.

- 1) Check that the Set Point is set to 60. If not, select the field and type 60.

- 2) If changing the Set Point, enter the new value and click Update. The heater will not go above 89 so entering a number higher will result in the heater permanently on attempting to reach the set point.

#### **5.1.4 Reaching steady state**

The system needs to be at steady state conditions inside of the chamber before a new sample could be taken. This required flushing out the chamber with the air from the lab bench. The following steps needed to be completed:

- 1) Fill up the bottle with new tap water to the line indicated on the bottle. This equates to approximately 200mL.
- 2) Screw on the lid of the bottle and ensure the air stone is completely submerged.
- 3) Open exit valve on the Hammond Box lid.
- 4) Open lab bench air line valve such that the handle is in line with the output nozzle.  
Check to see that the air stone created mild bubbles inside of the bottle.
- 5) Set the Analog Pressure Gauge to approximately 1 PSI. The needle edge should be in line with the first marker.
- 6) Place the Hammond Box lid on top of the Hammond Box chamber.
- 7) Screw the lid securely on with the four screws.

Once the lid was on, the operator should be able to feel a very light air flow moving out of the exit valve on the lid. The exit valve needed to be open otherwise pressure inside the chamber could build up and damage components and jeopardize the validity of future results.

The low flow rate from the air line into the chamber is favorable to the environment because it would minimize the amount of turbulent flow that may disturb the sensor output. A piece of

paper was necessary to be placed under the lid to help displace the incoming air and avoid the incoming stream of air from focusing onto the top of any one sensor. This paper could also help 'catch' any possible water droplets that formed from condensation which could fall into the chamber. The low flow rate accounted for minimal adjustments for when the air line was turned off and for when the sample was injected into the chamber. Increasing the flow rate made the raw sensor values increase, so turning off the airline would result in a larger change from the standard baseline.

It took approximately 90 minutes to reach steady state inside of the chamber. This time was required for the chamber to reach approximately 45°C during the setup. The temperature inside the chamber started off around room temperature (approx. 25°C) at the beginning and rose after the sensor heaters heated up. The Capture tab also displayed the temperature and humidity inside the chamber from two different locations. The values displayed were usually slightly different due to the fact that they were in different areas inside the box and that not all the sensors were being used. The humidity inside the chamber typically started off around 50% relative humidity when the temperature was close to room temperature. As the temperature increased the relative humidity dropped to between 17% and 25%. The graphical output displayed the environmental conditions and once both values flat-lined, it was accepted that steady state inside the chamber had been achieved. The sensor values also needed to be at a steady state and this was determined by looking at the change in raw sensor values over one minute. It was easiest to see if steady state had been achieved if the graphical output had been logging data and displaying everything since the beginning. A flat line indicating steady state was obvious to recognize due to the large response curve the sensors would initially show when heating up.



The vial heater module temperature was displayed at the very bottom of the Berry Punch user interface. It listed the set point, actual temperature and the difference from the set point. The actual temperature was typically within 0.2°C from the set point and this was acceptable to be considered steady state.

## **5.2 Sample Collection Methods**

Multiple methods were investigated to determine the best procedure to sample data accurately. The research investigated 4 different gas delivery methods that each allowed for different timed trial lengths (1 Minute to multiple Hours), various quantitative samples sizes (1 µL to 2ml), and multiple combinations of resistors for the sensors.

### **5.2.1 Procedure 1: Open Vial Heating Chamber**

The ‘Open Vial Heating Chamber’ procedure was a method to investigate if there was an advantage to evaporating some of the sample before letting the remaining contents of the vial flow into the chamber for analysis. This method was trialed because the vapor pressures and boiling points of the 6 different testing compounds had large variances. The Ethanol could potentially evaporate from the sample leaving only the remaining targeted compound. The following was the simplified method trialed for sample collection:

- 1) Allow for steady state from a very low flow rate.
- 2) The sample vial was then placed in the heating chamber and timer was started.
- 3) After a specific time interval (options listed below), the rubber stopper and septa were placed on top the heater block and the valve to the chamber was opened to allow sample to flow in.

- 4) The low flow rate from the air bench was kept on and flowed through the exit valve of the chamber. The sample flowed through the chamber for a pre-determined level of time.
- 5) All valves were then closed.
- 6) The data was saved after 500 seconds of sampling.
- 7) Start baseline recovery.

This method showed to be a suitable way to focus on the high vapor pressure compounds because the Ethanol had theoretically been evaporated away before the measurements began. It was experimented with the following different heating and flow times:

*Heating Times: 60s, 120s, 135s, 150s, 165s*

*Sample Flow Times: 120s, 180s*

By heating 5  $\mu$ L samples of 20% Ethanol ABV, it was determined how long it would take the heater to evaporate the Ethanol. After 165 seconds of heating, there was little to no Ethanol left to be detected by the sensors. Figure 26 through Figure 29 below show the response from the sensors when the heating chamber was allowed to evaporate the sample into the air for 120 to 165 seconds. After 120 seconds, Figure 26 shows that there was still a response from some of the sensors when detecting Ethanol, yet after 165 seconds Figure 29 shows hardly any response at all implying there was no more ethanol in the vial left to detect. A completely flat line from the sensors would indicate that no Ethanol was detected.

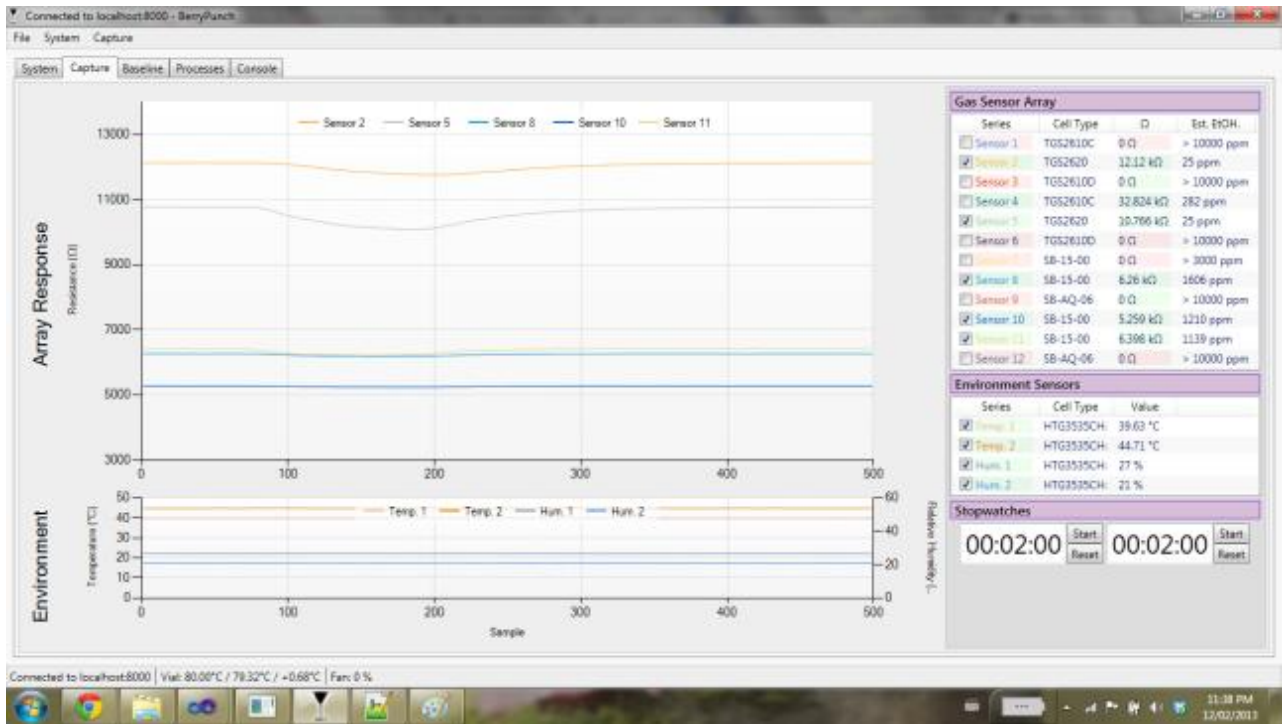


Figure 26: A 5µL Ethanol 20% ABV sample preheated at 80°C for 120 seconds sample response with 120 second data recording

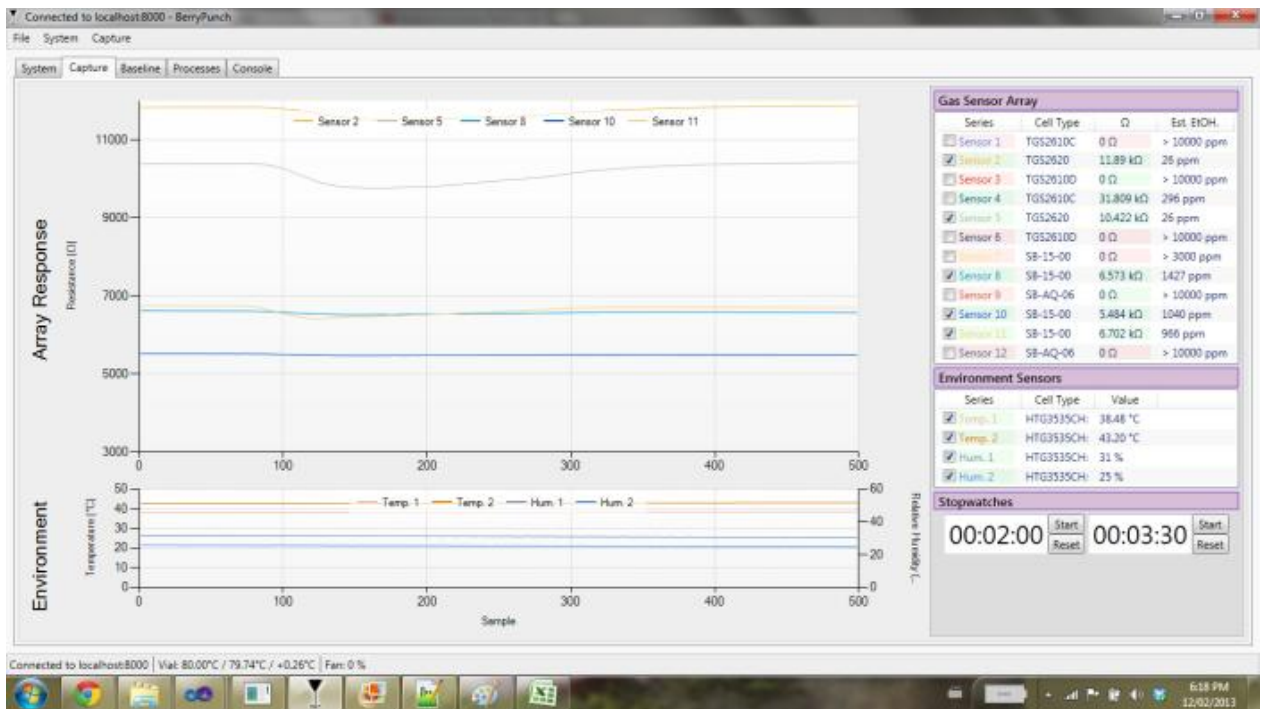


Figure 27: A 5µL Ethanol 20% ABV sample preheated at 80°C for 135 seconds sample response with 180 second data recording

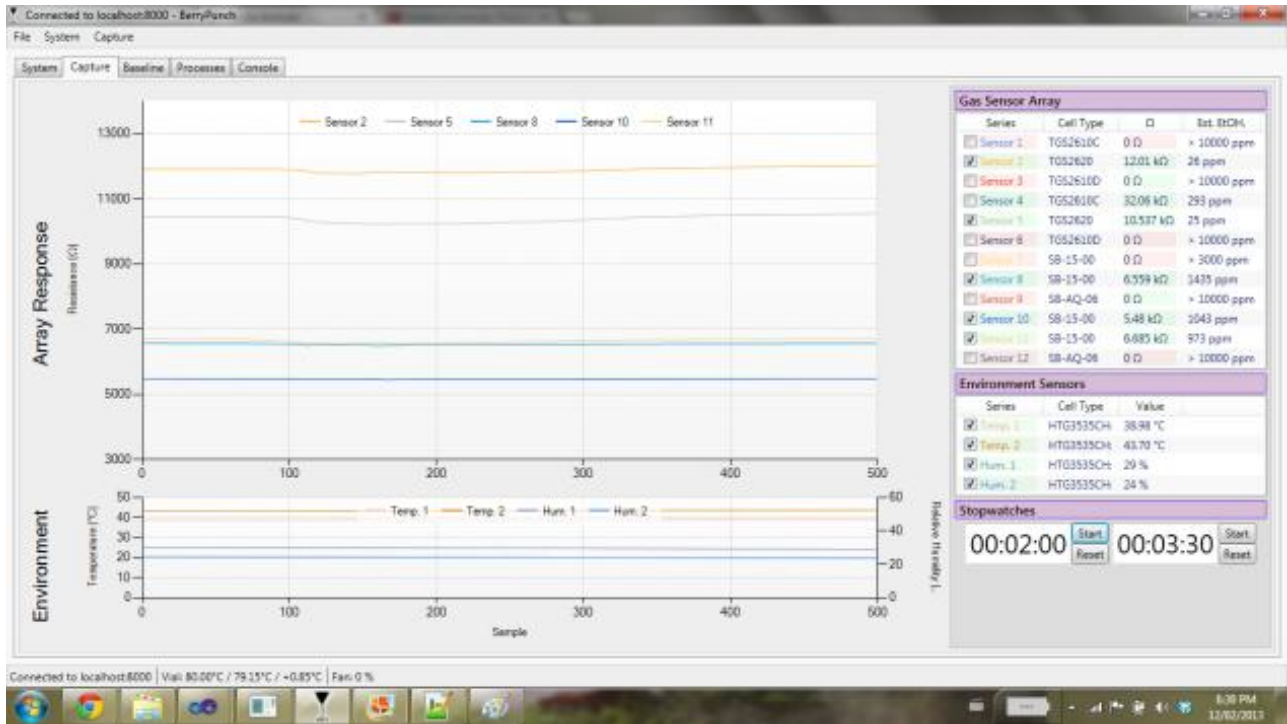


Figure 28: A 5µL Ethanol 20% ABV sample preheated at 80°C for 150 seconds sample response with 180 second data recording

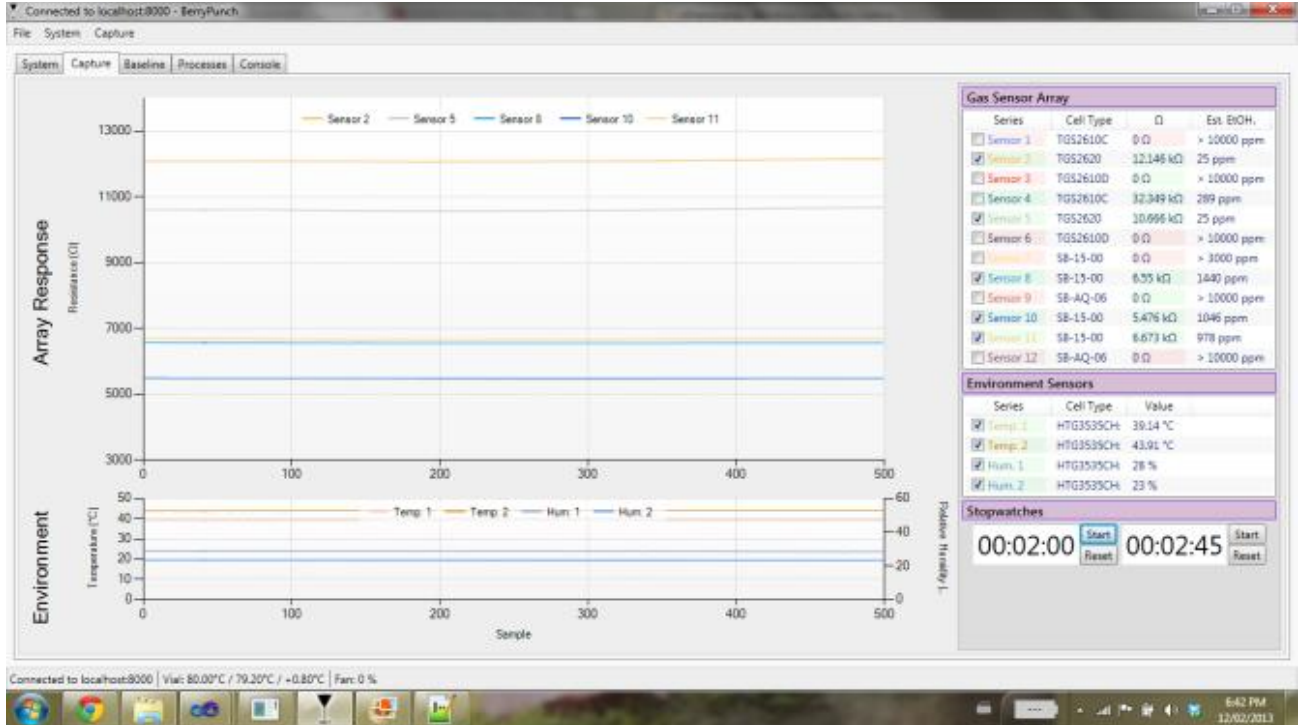


Figure 29: A 5µL Ethanol 20% ABV sample preheated at 80°C for 165 seconds sample response with 180 second data recording

### 5.2.2 Procedure 2: Immediate Sample Flow

The 'Immediate Sample Flow' procedure was trialed to investigate how the sensors responded to the sample as it was heated up while simultaneously evaporated into the chamber. This method could be used to determine how long it would take for the entire sample to evaporate and how long the odor would linger inside of the chamber. The following simplified procedure was used for the Immediate Open method:

- 1) Turn the clean air flow off.
- 2) Place 5  $\mu\text{L}$  sample in heater set at 80°C.
- 3) Place the rubber stopper and septa on top the heater block open the valve to the chamber to allow sample to flow in.
- 4) Close clean air inlet and outlet.
- 5) Wait for predetermined amount of time (options listed below).
- 6) Close the sample inlet.
- 7) Save Results after a total of 500 seconds has passed.

This method was used to determine how long it would take for the sensors to reach their steady state settling point by flat lining. The information could be used to understand how long future samples would be required to be taken for. It was experimented with the following different sample release times (time that the sample flowed into the chamber):

- 1) 60 seconds
- 2) 200 seconds
- 3) 360 seconds
- 4) Indefinitely (2000 seconds to 30 minutes)

The following graph in Figure 30 shows what happened when the sample flowed into the chamber for 30 minutes with all other valves closed. It showed that after approximately 450 seconds there was very little (if any) change in response from the sensors. This test was

important so that the sensor's steady state response could be compared to a sample that had been exposed to the chamber for a shorter period of time. This test would expose whether the sample would settle to the same steady state value if more time was allotted. A more aggressive response could potentially allow for an easier classification.

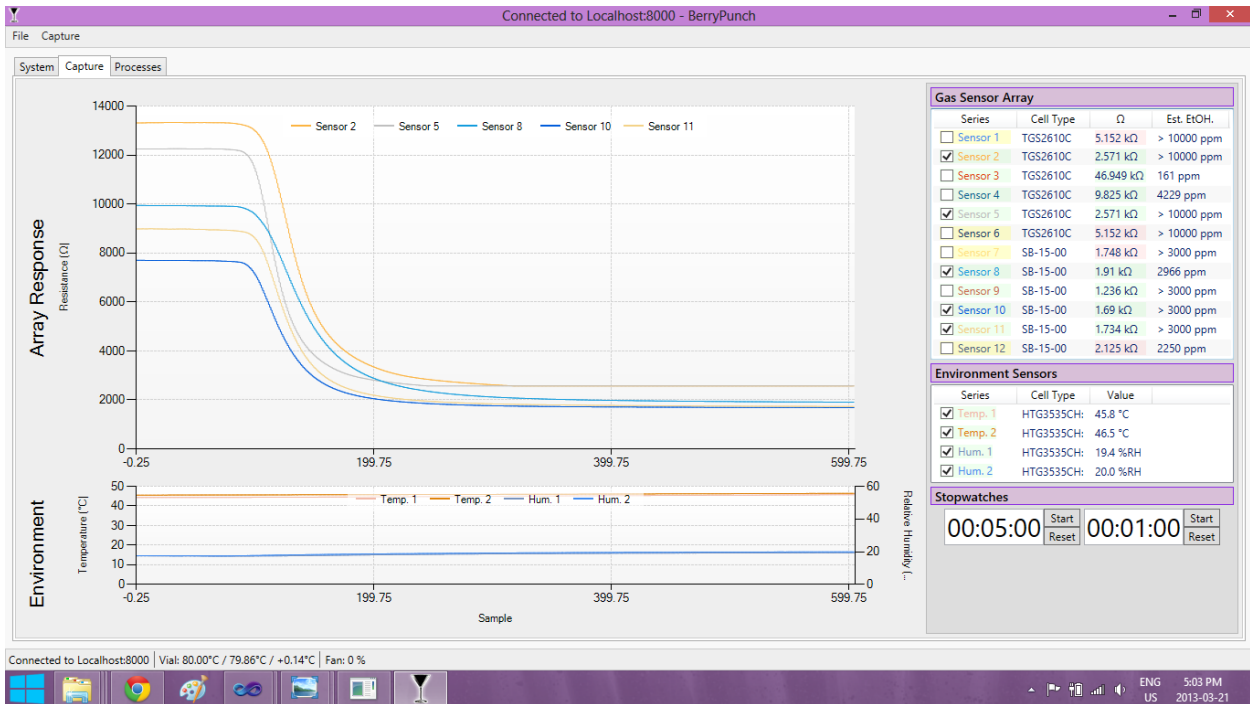


Figure 30: A 5µL Ethanol 20% ABV sample released into the chamber immediately and recorded until no response found

### 5.2.3 Procedure 3: No Air Flow during Baseline Recordings

The previous experiments had a 60 second initial baseline recorded while the clean air was flowing through the chamber. This experiment was designed to compare the effects of what happens when the samples flow into the chamber without clean air flowing being used for the 60 second baseline.

Once it was determined that steady state was achieved, the air inlet was turned off and the sample was released into the chamber with the exit valve open. The following simplified procedure was used to measure this method:

- 1) Turn the clean air flow off.
- 2) Place 5  $\mu\text{L}$  sample in heater set at 80°C.
- 3) The rubber stopper and septa were placed on top the heater block and the valve to the chamber was opened to allow sample to flow in.
- 4) Close air inlet, leave air outlet open.
- 5) Let sample flow into the chamber for determined time (listed below).
- 6) Close sample inlet.
- 7) Save Results after a total of 600 seconds has passed.

The sample was let into the chamber for the following different lengths of time:

*Sample Flow Times: 180s, 240s, 300s, 360s*

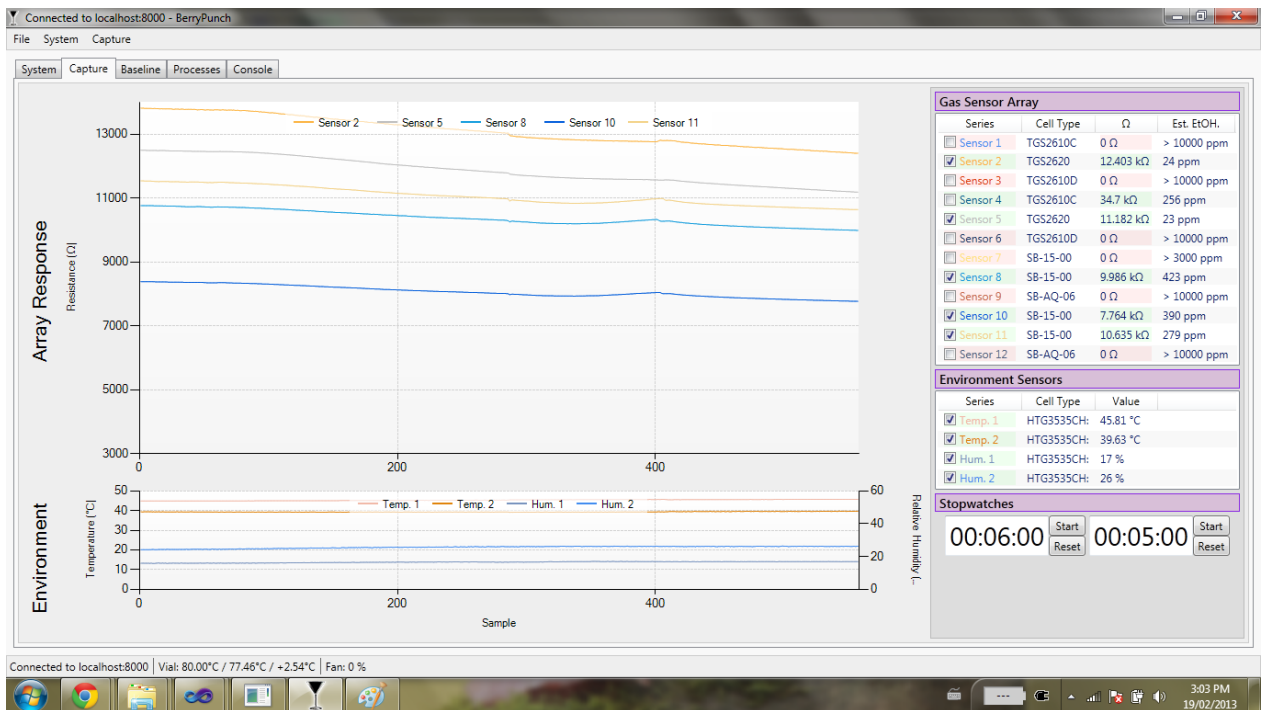


Figure 31: No air flow when reading sample: A 5  $\mu\text{L}$  Sample with Ethanol at 20% ABV for 360 seconds

This method was not considered a successful method to analyze data. Multiple problems were easily noticed from the screen shot result above in Figure 31. The 60 second initial baseline was not flat which provided a poor reference point. The output after 360 seconds also indicated a disturbance in the chamber when closing the valve. After all the valves were closed the sensors were still not able to display a final settling point and showed modest signs of changing in the near future. This method showed that it would take a long time to record each sample and that was not a desirable trait of future sample collections.

#### **5.2.4 Procedure 4: No air flow when reading a trapped sample**

The ‘no air flow when reading a trapped sample’ method was a procedure designed to record the samples in the chamber with minimal other disturbances. It required the chamber to be at steady state for an extended period of time before allowing a sample to be measured. Once the sample inlet valve was opened for a determined level of time (options listed below), then all of the valves inside the chamber were to be closed. A simplified procedure is listed below

- 1) Turn the clean air flow on, leave the outlet flow open.
- 2) Place 5  $\mu\text{L}$  sample in heater set at 80°C for 6 minutes.
- 3) Place septa and cork onto heater block after the 6 minutes.
- 4) Turn off air flow, close outlet valve, open sample inlet valve.
- 5) Let sample flow into chamber for 5 minutes.
- 6) Close Sample Valve (all valves closed in chamber)
- 7) Allow sample to settle until 600 seconds mark.
- 8) Save Results.

This method proved to be one of the most consistent methods. When a sample was trialed the sensors responded very reliably and settled out after the valve was close. Figure 32 shows how



the sensors responding to Ethanol after being heated for 50 seconds, and letting it flow into the chamber for an additional 120 seconds. Repetitive trials showed similar results.

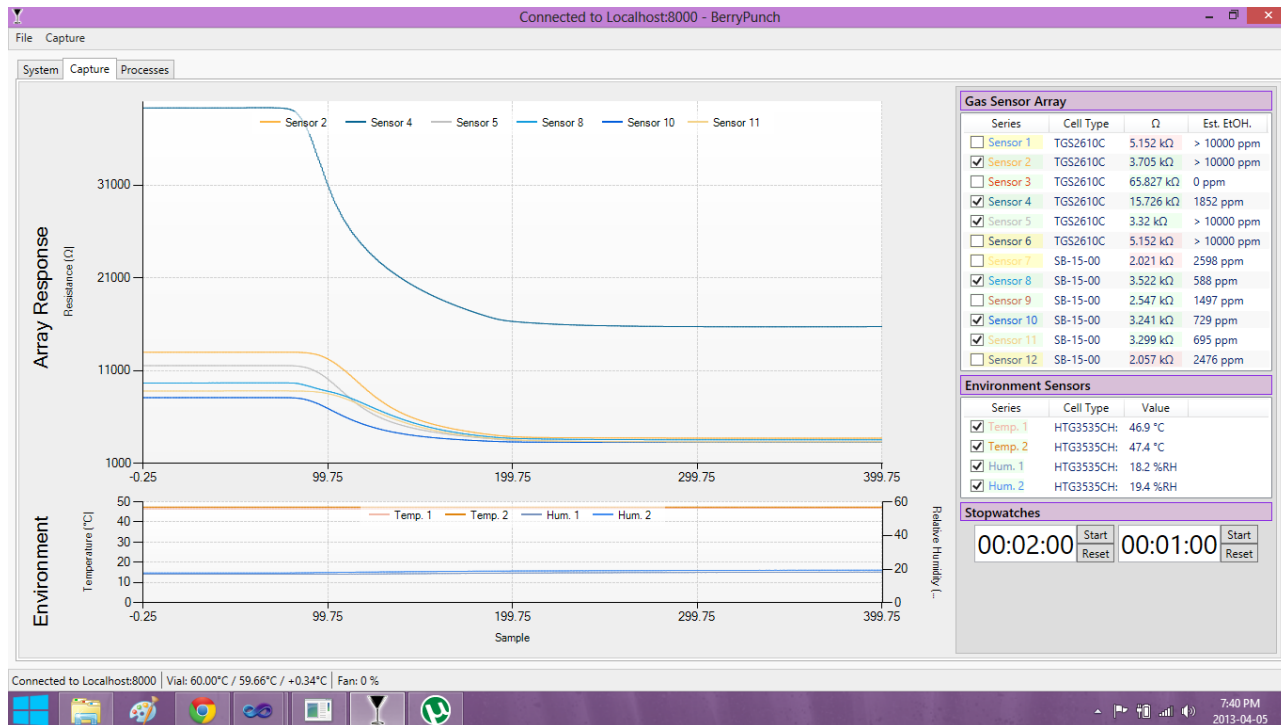


Figure 32: A 5 $\mu$ L Sample with Ethanol at 20% ABV response when in chamber 120 seconds and no airflow.

This method proved to be very useful because the sensors behaved in an expected manner. This meant that the response behaved well (without disturbances), and that the sensors eventually settled to a steady state position. The challenge with this method was that the sensors would drift initially when an empty vial was released into the chamber. A possible explanation for this occurrence could be the change in hot air from the heating chamber moderately affecting the sensor response.

### 5.3 Fan Speed and Air Flow Rate

The speed that the fan operated at and the rate that the clean air flowed into the chamber had a large impact on the performance of the electronic nose. The turbulent air created by the fan

proved to affect the measurements in a negative way. It was determined that the measurements were more reliable with the fan off and future samples were to not utilize the fan.

The air inlet flow was used to flush out the chamber. Higher flow rates would clear out the chamber faster; however adjusting the analog controller on the lab bench was prone to human error and it was very sensitive. Changing the flow rate would also adjust the level of humidity and temperature inside the chamber. Once the air flow control was turned off and all the valves were closed, the sensors would typically sense a lower resistance and trend downwards for hours and not settle. A floating baseline would cause many problems. The final method used to record data would feature a 60 second baseline with the air inlet open at a very low flow rate, and would also turn off simultaneously when the sample inlet was opened. This resulted in the baseline always appearing flat.

#### **5.4 Summary**

The system used to record samples has been outlined and presented in this chapter. Four procedures were thoroughly tested and analyzed which determined the best method for future samples to be taken consistently. Section 5.2.4 proved to have been the most reliable method where the evaporated sample was enclosed into the sensing chamber. Large amounts of testing also showed the most effective ways to use the analog air flow controller and also that the fan was no longer to be used.

## Chapter 6

### 6 Results

The results from my research are presented in this chapter. They cover the finalized sample collection procedure, and an analysis of the data collected. The electronic nose was able to successfully log and respond to the presence of Ethanol, Ethyl Acetate, and Isopropyl Alcohol. Features were extracted from the signal response of 7 sensors and then used as inputs into a back propagating neural network classifier.

#### 6.1 Procedure

The procedure was an essential component to the overall design of the electronic nose. It needed to be extremely consistent to be able to reliably compare each trial. Multiple sample preparation methods were presented in the previous chapter to see which qualitative features were ideal. These findings were used to create the final procedure which would focus on repeatability and consistency. The maximum amount of sample that could be used was limited to the vial size at 2mL. To minimize the amount of the sample that evaporated during preparation, it would not be prepared until the chamber was at steady state and ready for analysis. A 10  $\mu$ L glass needle syringe was cleaned with water by siphoning clean water multiple times. It was dried off and then used to acquire the designated amount from each sample.

The procedure started when steady state inside of the chamber had been reached. Unfortunately the baseline was not the same on a daily basis. Steady state inside the chamber was considered acceptable once the change over 200 seconds was less than 0.5% from the previous sample. It took approximately 90 minutes to reach it the first time of the day because the sensors needed to warm up. Steady state took approximately 30 minutes for each sample after setup.

The procedure required many manual steps to be taken, and optimal results occurred once the operator was able to be as systematic as possible. Many of the steps required the following step to be taken immediately after. An ideal system would be entirely automated with electronic valves and processes. The steps to record one sample are as follows:

- 1) Wait until steady state.
- 2) Reset Capture on the screen. Capture (beside File) - > Reset Capture. \*\*

\*\* It is important to reset the capture initially because the system lags in the reset if more than 1000 samples are currently displayed on the screen. Clearing the history before allows for a smooth reset the following time.

- 3) Prepare sample.
- 4) Create the 1 minute baseline reference as fast as possible in this order (expected time to complete steps a. to e. was approximately 4 seconds):
  - a. Reset Capture on the screen. Capture (beside File) -> Reset Capture.
  - b. Start the 1:00 Timer.
  - c. Place vial (with sample) inside heating chamber.
  - d. Place septa and rubber stopper over heating chamber hole.
  - e. Press PrtSc to save an image of the screen.
  - f. File the image for self reference.
- 5) After the 1 minute timer reached zero, a sound notification was announced from the computer. At this time the sample was released into the chamber by following these steps as fast as possible in this order (expected time to complete steps a. to d. is approximately 2 seconds):

- a. Start the 4:00 Timer.
  - b. Completely close lab bench air line valve.
  - c. Completely close air exit valve on the lid of the Hammond Box.
  - d. Completely open the sample inlet valve from the vial heater module.
- 6) During the 4 minute wait, record the baseline sensor values for all the sensors being used in the 'Sensor Baseline Starting Values.xlsx' file. Also record any notes about the sample as well as the time, temperature and weather outside (from [theweathernetwork.com](http://theweathernetwork.com)).
- 7) After the 4 minute timer reaches zero, a sound notification was announced from the computer. The sample inlet valve was then closed. The graphical interface should show that 300 seconds had passed. \*\*Remove the sample from the chamber to minimize the risk of any remaining sample to leak into the chamber.
- \*\*The sample vial will be hot and should be handled with care.
- 8) With all valves closed inside the chamber, wait another 100 seconds.
- 9) Once the graphical output shows the sample number 400 press *PrtSc* to save an image of the screen for your personal records.
- 10) Save the sensor data:
- a. Click Capture (beside File) -> Export Data.
- 11) Once the export data is working (the screen will say 'Exporting # of Total Samples') that will mean the data will be successfully saved, and the baseline can start to recover back to normal:
- a. Open the Hammond Box lid exit valve completely.

- b. Open the lab bench air line valve such that the handle is in line with the nozzle.
- 12) Save the screen capture image for your records as the same name as the data you are exporting.
- 13) Save the Excel file with the old Microsoft Excel format (.xls) so that it can be opened in MATLAB.
- 14) Wait until the baseline is achieved. This typically takes 1800 seconds.

Leaving the graphical output on the screen was beneficial because it showed the relative change over time, and would allow the user to see when the baseline was back to the 60 second reference that the previous sample last started at. Over the course of one day, the baseline would fluctuate, and it was important that the baseline remained as flat as possible for future sample collection.

## **6.2 Sample Collection Accuracy**

The low concentrations of products provided by Pernod-Ricard proved to be very difficult to differentiate between due to the inherent environmental conditions the electronic nose would experience from a day to day basis. The baseline value fluctuated extensively within a 24 hour period and even larger differences were found when trialing samples after a week's time. All of the sensors experienced large fluctuations from a stable baseline value over the course of 24 hours. Over the course of the sample period, the 7 sensors used had a minimum of 8% change from the average baseline value and a maximum change of 31%. Overall the average fluctuation from the sensors baseline was approximately 23.7%. The fluctuating baseline made results appear incomparable. The air to clean the chamber came from the lab bench on the 3<sup>rd</sup> floor of the Thornborough Engineering building. This air supply originated from a common source that

was distributed throughout many buildings at the University and it was assumed there may have been compressor oil or other contaminants embedded into the air supply. Weather conditions may have also been a factor. Sensor steady state values, the sensing chamber temperature and humidity levels as well as the external environment conditions were recorded for investigation over multiple days and are displayed in ‘*Appendix B – Sample Initialization Conditions*’ Table 20, Table 21, and Table 22. Unfortunately there was no correlation discovered between environmental conditions and the response from the sensors.

Over 300 samples were recorded with the electronic nose and it took approximately 1 hour on average to complete each sample. This lengthy sampling process investigated dozens of methods to record data, each with dozens of different sensor resistors, and sample size combinations. Seven of the 12 available sensors in the chamber were used for analysis. Figure 33 and Figure 34 below show how 25 unique trials compared to each other over the course of one month. The top left flat section of the graph represents the 60 second baseline recording before the sample was released into the chamber. It is important to note the large differences in this baseline which ideally should all start at the exact same value. The upper extreme for the sensor 2 baseline starting point was approximately 13.831K $\Omega$ , and the lower bound baseline was around 12.037K $\Omega$ . The top right shows a legend identifying the day that the sample was collected as well as what the sample consisted of.

Table 12 below highlights the details of the 25 samples that are graphed. These 25 samples were all taken within a 3 day period and had the same sensor resistors selected when being analyzed. The list includes combinations of Ethanol with Ethyl Acetate totaling 5 $\mu$ L as well as smaller quantities of the samples for comparing settling points. The Ethanol samples were 20% ABV, but the samples of Ethyl Acetate, and Isopropyl Alcohol were 100%, and 99% respectively.

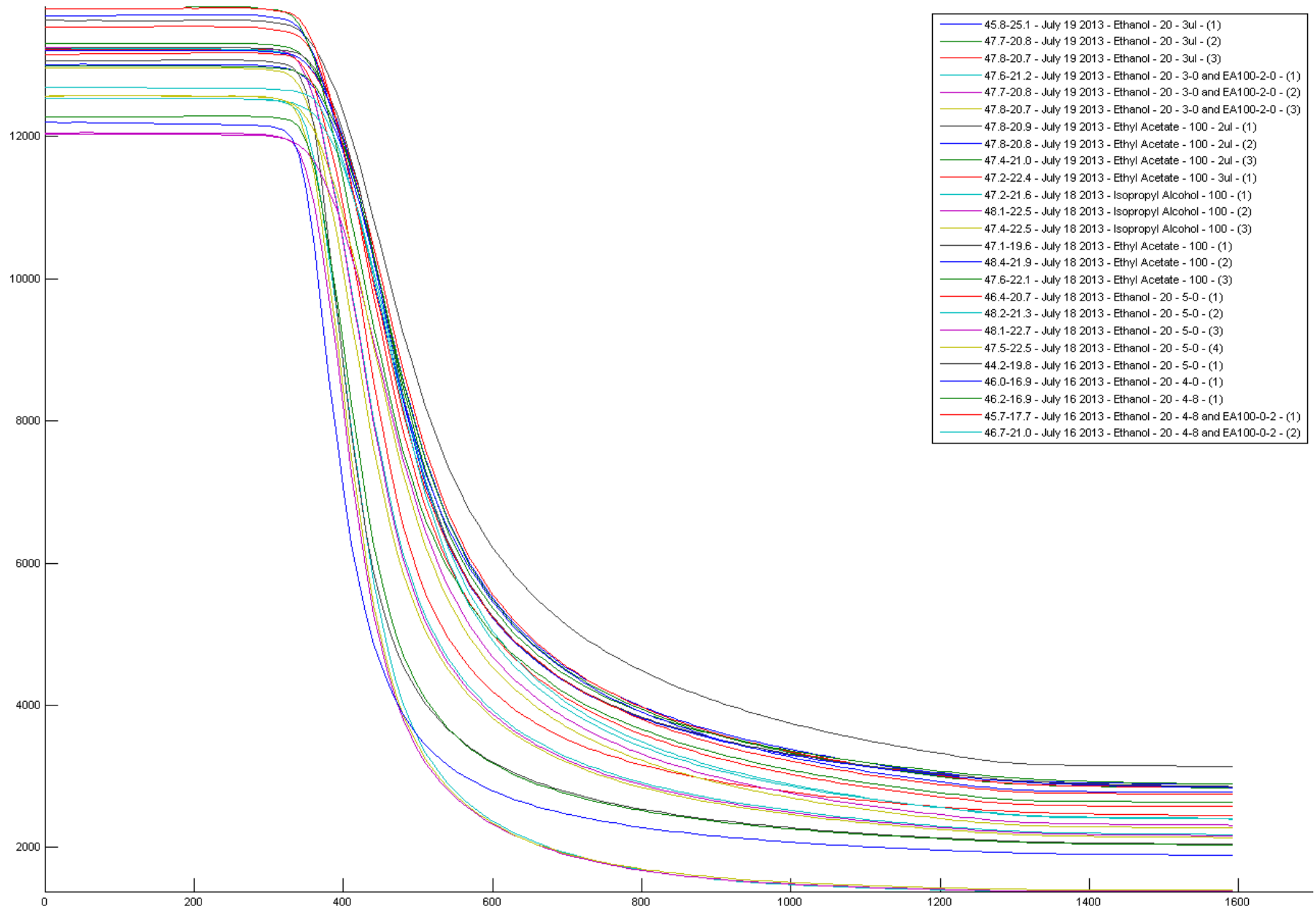


Figure 33: Sensor 2 Comparable Sample Data Recordings - Resistance



Sensor. 3 - FIG TGS2610 - 164tf #15

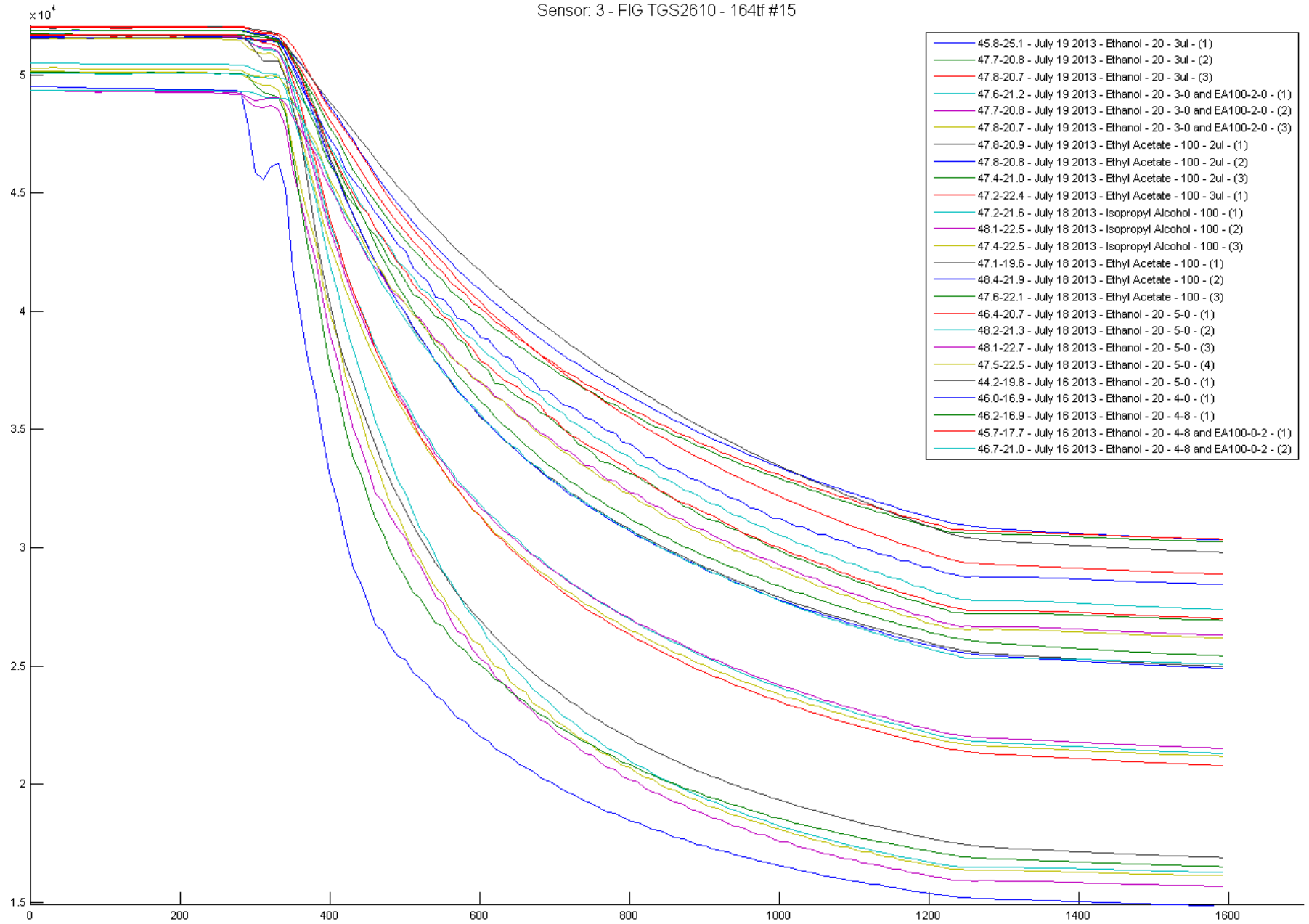


Figure 34: Sensor 3 Comparable Sample Data Recordings - Resistance

Sensor: 3 - FIG TGS2610 - 164lf #15

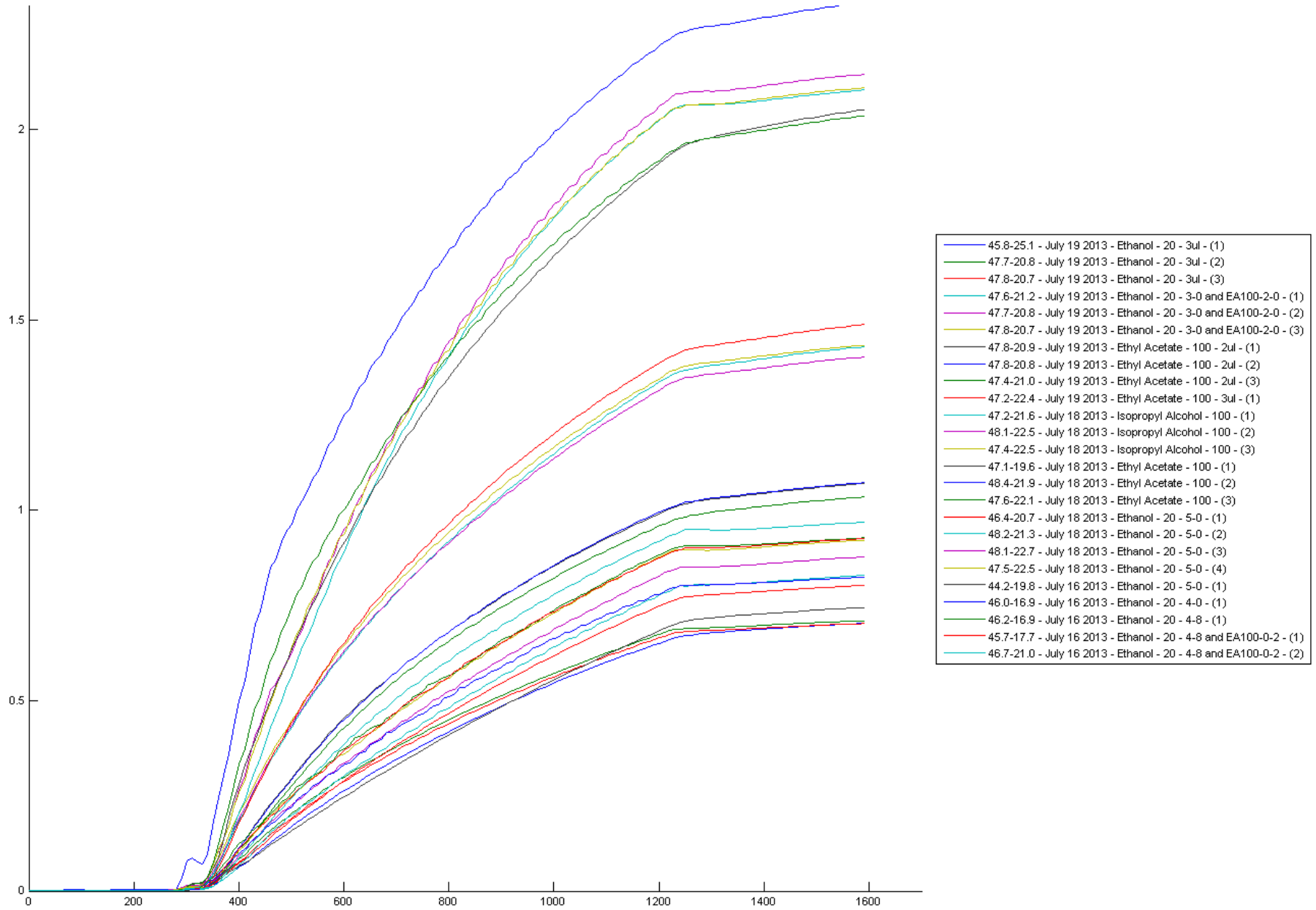


Figure 35: Sensor 3 Comparable Sample Data Recordings - Normalized Conductance

<b>ID</b>	<b>Date Sample Taken</b>	<b>Total Sample Size (µL)</b>	<b>Ethanol (µL)</b>	<b>Ethyl Acetate (µL)</b>	<b>Isopropyl Alcohol (µL)</b>	<b>Filename</b>
1	July 19 2013	3	3	0	0	<i>July 19 2013 - Ethanol - 20 - 3ul - (1).xls</i>
2	July 19 2013	3	3	0	0	<i>July 19 2013 - Ethanol - 20 - 3ul - (2).xls</i>
3	July 19 2013	3	3	0	0	<i>July 19 2013 - Ethanol - 20 - 3ul - (3).xls</i>
4	July 19 2013	5	3	2	0	<i>July 19 2013 - Ethanol - 20 - 3-0 and EA100-2-0 - (1).xls</i>
5	July 19 2013	5	3	2	0	<i>July 19 2013 - Ethanol - 20 - 3-0 and EA100-2-0 - (2).xls</i>
6	July 19 2013	5	3	2	0	<i>July 19 2013 - Ethanol - 20 - 3-0 and EA100-2-0 - (3).xls</i>
7	July 19 2013	2	0	2	0	<i>July 19 2013 - Ethyl Acetate - 100 - 2ul - (1).xls</i>
8	July 19 2013	2	0	2	0	<i>July 19 2013 - Ethyl Acetate - 100 - 2ul - (2).xls</i>
9	July 19 2013	2	0	2	0	<i>July 19 2013 - Ethyl Acetate - 100 - 2ul - (3).xls</i>
10	July 19 2013	3	0	3	0	<i>July 19 2013 - Ethyl Acetate - 100 - 3ul - (1).xls</i>
11	July 18 2013	5	0	0	5	<i>July 18 2013 - Isopropyl Alcohol - 100 - (1).xls</i>
12	July 18 2013	5	0	0	5	<i>July 18 2013 - Isopropyl Alcohol - 100 - (2).xls</i>
13	July 18 2013	5	0	0	5	<i>July 18 2013 - Isopropyl Alcohol - 100 - (3).xls</i>
14	July 18 2013	5	0	5	0	<i>July 18 2013 - Ethyl Acetate - 100 - (1).xls</i>
15	July 18 2013	5	0	5	0	<i>July 18 2013 - Ethyl Acetate - 100 - (2).xls</i>
16	July 18 2013	5	0	5	0	<i>July 18 2013 - Ethyl Acetate - 100 - (3).xls</i>
17	July 18 2013	5	5	0	0	<i>July 18 2013 - Ethanol - 20 - 5-0 - (1).xls</i>
18	July 18 2013	5	5	0	0	<i>July 18 2013 - Ethanol - 20 - 5-0 - (2).xls</i>
19	July 18 2013	5	5	0	0	<i>July 18 2013 - Ethanol - 20 - 5-0 - (3).xls</i>
20	July 18 2013	5	5	0	0	<i>July 18 2013 - Ethanol - 20 - 5-0 - (4).xls</i>
21	July 16 2013	5	5	0	0	<i>July 16 2013 - Ethanol - 20 - 5-0 - (1).xls</i>
22	July 16 2013	4	4	0	0	<i>July 16 2013 - Ethanol - 20 - 4-0 - (1).xls</i>
23	July 16 2013	4.8	4.8	0	0	<i>July 16 2013 - Ethanol - 20 - 4-8 - (1).xls</i>
24	July 16 2013	5	4.8	0.2	0	<i>July 16 2013 - Ethanol - 20 - 4-8 and EA100-0-2 - (1).xls</i>
25	July 16 2013	5	4.8	0.2	0	<i>July 16 2013 - Ethanol - 20 - 4-8 and EA100-0-2 - (2).xls</i>

Table 12: Sample Comparison Details

The Berry Punch software automatically logged the sensors resistance, and inverting the values would show the conductance of the response and this modification had proven to be beneficial for analysis. Figure 35 shows the baseline start normalized to zero by calculating the average baseline, and adding the difference to each sensor value. This modification resulted in a much larger spectrum of settling locations on the right side of the graphs. Figure 34 above shows clear starting positions for the baseline which translates into different days of taking samples. The settling location tended to differentiate into the array of chemicals despite the variance in starting baseline.

### **6.3 Feature Extraction**

The 25 samples were analyzed and features were extracted from them to be used as inputs into a neural network. The following 7 features listed in Table 13 below were extracted from the sensor responses. Other features had been investigated; however the neural network would not perform satisfactory classifications when using the features.

<b>Feature Identification</b>	<b>Definition</b>
<i>Maximum Slope</i>	A function created to find the maximum change in the sensor response over a set number of samples. For this specific design, the maximum change was found over 10 samples.
<i>Maximum Slope Location</i>	A reference to the above Maximum Slope feature and the sensor sample number that it was found at.
<i>Average of the Last 25 Samples Original Reading</i>	The last 25 sensor values of the response from each sensor were averaged where the sample had achieved steady state.
<i>Average of the Last 25 Samples modified to show the Zeroed Conductance value</i>	All sensor responses were adjusted to show the conductance (instead of Resistance). The response was then normalized to the average of all 25 samples and the difference was added to the original signal. The last 25 sensor values were then averaged and used to represent this feature.
<i>The 600<sup>th</sup> Sample</i>	The 600 <sup>th</sup> sample from the sensor response.
<i>The 800<sup>th</sup> Sample</i>	The 800 <sup>th</sup> sample from the sensor response.
<i>The 1000<sup>th</sup> Sample</i>	The 1000 <sup>th</sup> sample from the sensor response.

**Table 13: Feature Extraction Table**

## 6.4 Neural Network Classification

The back propagating neural network created used a momentum rate of 0.95 and a floating learning rate that began training at 0.4. As the average training error of the network decreased, the learning rate decreased as well. The network started with a higher learning and momentum rate to attempt to avoid the system becoming stuck in a local minimum or local maximum. As the average training error lowered, the learning rate lowered to try to fine tune the parameters of

the system. The change in learning rate with respect to the average training error is listed below in Table 14.

<b>Average Training Error</b>	<b>Learning Rate</b>
$ATE > 0.30$	0.4
$0.30 \geq ATE > 0.25$	0.2
$0.25 \geq ATE > 0.15$	0.1
$0.15 \geq ATE > 0.10$	0.05
$0.10 \geq ATE > 0.05$	0.03

**Table 14: Learning Rate Adjustment**

The network completed training once one of the following three criteria was met:

1. The maximum number of epochs was met.
2. The average maximum training error was less than 0.01.
3. The maximum training error was less than 0.01

The 25 samples (listed in Table 12) used were randomized such that the training and testing data changed each trial. The first twenty samples in the randomized order were used as the training data, and the remaining five were used to test the network. This randomization did create the risk that all three samples of the same concentration could all be in the testing stage and therefore the network would not learn about their qualities and instead only test it. This unique case would lead to a poor overall classification but it was important to investigate if the network could still determine what chemical was being analyzed based off of the input features.

The 7 features extracted from each of the 7 sensors created the input array for the network. These 49 inputs would be classified to determine 3 possible outputs. The 3 outputs were a measure of the amount of  $\mu\text{L}$  of Ethanol, Ethyl Acetate, and Isopropyl Alcohol that were found in each sample. Each output layer node calculated a value between 0 and 1, and a value of 1 indicated that there was 5  $\mu\text{L}$  of that chemical detected. If the output of a single node was 0.6 that implied that 3  $\mu\text{L}$  of that chemical was detected. An example of the output is presented below in Table 15.

Test Number	Output Node	Output Value	Correct Value	Absolute Error	Total Error	Output Guess ( $\mu\text{L}$ )	Actual Amount ( $\mu\text{L}$ )	Actual Error ( $\mu\text{L}$ )
1	1	0.284344	0	0.284344	0.357951	1.42172	0	1.42172
	2	0.671293	0.6	0.071293		3.356465	3	0.356465
	3	0.002314	0	0.002314		0.01157	0	0.01157
2	1	0.915846	0.6	0.315846	0.316332	4.57923	3	1.57923
	2	0.00047	0	0.00047		0.00235	0	0.00235
	3	0.000016	0	0.000016		0.00008	0	0.00008
3	1	0.994458	1	0.005542	0.009039	4.97229	5	0.02771
	2	0.003447	0	0.003447		0.017235	0	0.017235
	3	0.00005	0	0.00005		0.00025	0	0.00025
4	1	0.04574	0	0.04574	0.161772	0.2287	0	0.2287
	2	0.285417	0.4	0.114583		1.427085	2	0.572915
	3	0.001449	0	0.001449		0.007245	0	0.007245
5	1	0.00246	0	0.00246	0.017165	0.0123	0	0.0123
	2	0.006036	0	0.006036		0.03018	0	0.03018
	3	0.991331	1	0.008669		4.956655	5	0.043345
<b>Average Error:</b>				0.0574839		<b>Average Actual Error (<math>\mu\text{L}</math>):</b>		0.28742
<b>Total Error:</b>				0.862259				

Table 15: Neural network output classification for 5 samples

The output shows the results of 5 testing samples. Error was calculated by taking the absolute value of difference between the correct values from the output values. The final 3 columns show a representation of what the actual values in  $\mu\text{L}$  were calculated to be. This example below shows a range of tests that include 3 partial samples (samples less than 5  $\mu\text{L}$ ) as well as 2 pure

samples. Test number 1 in the list highlights the networks ability to learn the appropriate value of Ethyl Acetate despite that there were no identical samples that the network could train from. A majority of the actual errors in  $\mu\text{L}$  show that the classifier was able to very accurately determine what the chemical was. The output is a very respectful result considering human error in creating the samples was a possibility when working with such low amounts of each chemical.

The network tried multiple configurations to test the data. To maximize performance, the network cycled through different architectures by varying the number of hidden nodes in the middle layer and adjusting the number of epochs. The number of hidden nodes cycled between 5 and 50 in 5 node step increments. Each configuration was trialed with 1000, 1500, and 2000 epochs. Table 16 below shows the result of testing each configuration 20 times. It shows that the configuration with the lowest average error and with the lowest max error was with 45 hidden layer node architecture trained over 1000 epochs. The values in the table represent the total error between the 5 testing data. Each of the 5 tests could have a maximum error of 3, and thus between all 5 the worst possible error could be 15.



<b>Epochs</b>	<b>Hidden Nodes</b>	<b>Average Error</b>	<b>Min Error</b>	<b>Max Error</b>
<i>1000</i>	<i>5</i>	3.2	1.501	4.958
<i>1500</i>	<i>5</i>	3.136	1.098	7.185
<i>2000</i>	<i>5</i>	3.146	0.59	6.196
<i>1000</i>	<i>10</i>	3.739	0.817	5.223
<i>1500</i>	<i>10</i>	2.632	0.817	6.601
<i>2000</i>	<i>10</i>	2.625	0.593	4.694
<i>1000</i>	<i>15</i>	2.578	0.624	4.567
<i>1500</i>	<i>15</i>	2.611	0.838	5.47
<i>2000</i>	<i>15</i>	2.039	0.707	4.519
<i>1000</i>	<i>20</i>	2.733	0.986	4.578
<i>1500</i>	<i>20</i>	2.745	0.997	6.114
<i>2000</i>	<i>20</i>	2.484	0.724	6.134
<i>1000</i>	<i>25</i>	2.182	0.456	4.946
<i>1500</i>	<i>25</i>	2.216	0.597	4.547
<i>2000</i>	<i>25</i>	2.137	0.388	5.094
<i>1000</i>	<i>30</i>	2.331	0.817	4.246
<i>1500</i>	<i>30</i>	2.687	0.904	4.82
<i>2000</i>	<i>30</i>	2.138	0.604	4.76
<i>1000</i>	<i>35</i>	2.266	0.712	5.276
<i>1500</i>	<i>35</i>	2.028	1.012	5.458
<i>1000</i>	<i>40</i>	2.562	0.953	6.83
<i>1500</i>	<i>40</i>	2.393	0.776	6.921
<i>1000</i>	<i>45</i>	1.839	0.722	2.838
<i>1500</i>	<i>45</i>	2.406	0.542	4.852
<i>1000</i>	<i>50</i>	2.346	0.944	4.893
<i>1500</i>	<i>50</i>	2.173	0.71	6.376

Table 16: Neural Network Architecture Results

Table 16 was summarized by the number of epochs and shown below in Table 17. It clearly shows that the longer the network was trained the better the overall result was.

<b>Epochs</b>	<b>Average Error</b>	<b>Min Error</b>	<b>Max Error</b>
<i>1000</i>	2.578	0.456	6.830
<i>1500</i>	2.503	0.542	7.185
<i>2000</i>	2.428	0.388	6.196

Table 17: Neural Network Epoch Summary Table

Table 18 below highlights a summary of using each different hidden node configuration. The results implied that more hidden nodes improved the performance of the system.

Hidden Nodes	Average Error	Min Error	Max Error
5	3.161	0.590	7.185
10	2.999	0.593	6.601
15	2.409	0.624	5.470
20	2.654	0.724	6.134
25	2.178	0.388	5.094
30	2.385	0.604	4.820
35	2.147	0.712	5.458
40	2.478	0.776	6.921
45	2.123	0.542	4.852
50	2.260	0.710	6.376

Table 18: Neural Network Hidden Node Summary Table

The 45 node hidden layer architecture appeared to produce the most consistent results. This architecture (Figure 36 below) was then trialed to determine an optimal number of epochs to train the network for. Overtraining a network could result in a system that cannot handle new data well and classifies poorly.

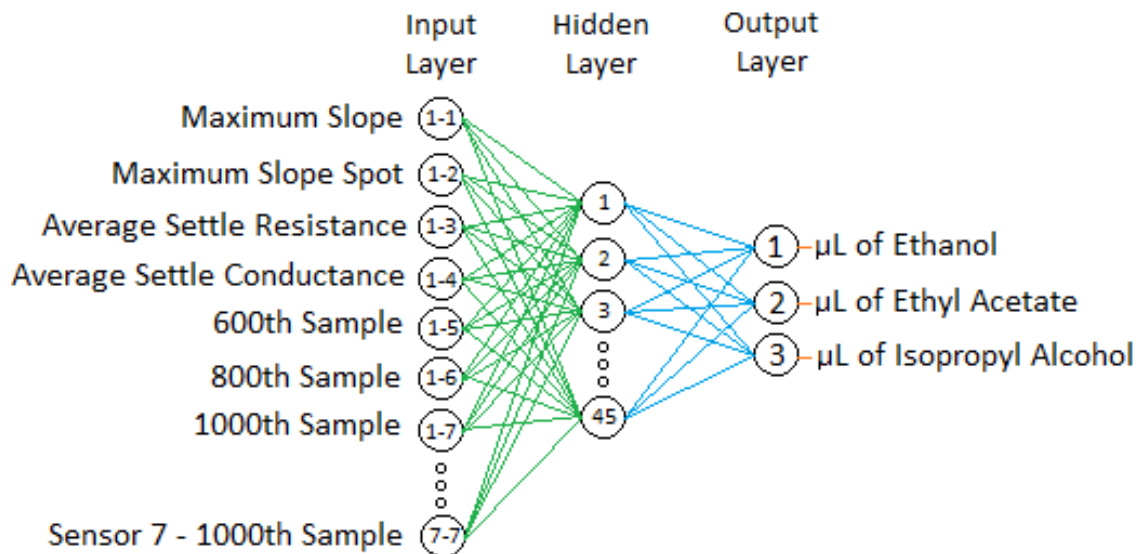


Figure 36: Neural Network Architecture

This network architecture above was trialed 100 times for 1000, 2000 and 3000 epochs. Table 19 below summarizes the results. This table totals the number of times the classification error at each output node fell within a specific range. A very low percentage of trials had completely incorrect classification error of 1 (approx 1%). The overall average output error for classification was decreased as the number of epochs increased. The best resulting classification occurred with 3000 epochs with an average error at each output node of 0.1247. This value means that the network could classify a sample consisting of multiple alcohols to within approximately 12.5% error in chemical composition. A majority of the outputs (almost 67% with 3000 epochs) were able to classify the alcohol with less than 10% error.

Classification Error	Epochs		
	3000	2000	1000
CE = [0, 0.1)	1004	988	906
CE = [0.1, 0.2)	158	159	166
CE = [0.2, 0.3)	96	98	113
CE = [0.3, 0.4)	98	103	130
CE = [0.4, 0.5)	54	46	47
CE = [0.5, 0.6)	35	36	41
CE = [0.6, 0.7)	11	19	29
CE = [0.7, 0.8)	7	19	15
CE = [0.8, 0.9)	21	18	14
CE = [0.9, 1)	16	14	39
<b>Total</b>	1500	1500	1500
<b>Individual Output Average Error</b>	0.1247	0.1293	0.1587
<b>5 Sample Average Error</b>	1.8708	1.9665	2.3807

Table 19: Classification Error for 1000, 2000, and 3000 epochs for Individual Outputs

The total error of the output nodes was summed for each test and is graphed below in Figure 37. The graph compares the frequency of the output classification error over 3000 epochs and is essentially a different way to visualize the data from Table 19. The maximum output error for this bar graph is 3 and the response shows that a completely incorrect classification did not occur. All 500 unique tests completed from the 100 randomized rounds of testing the neural network are displayed in this figure. It can be observed that a majority of the tests resulted in the output error totaling less than 0.1%.

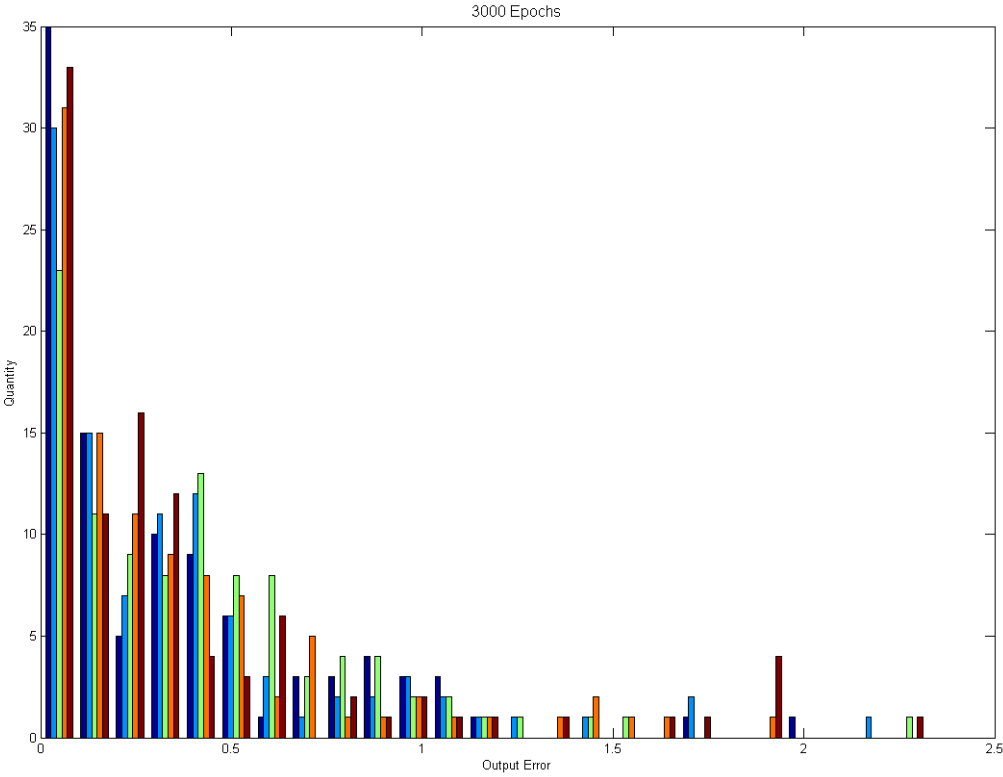


Figure 37: Neural Network Output Error Graph

## **6.5 Summary**

The results show that the neural network was successfully able to classify the samples to within 12.5 % (error on average) of the actual concentration. These values are quite acceptable given the state of the initial data set. The neural network had to compensate for a large floating baseline and for the limited amount of data for some samples. The samples with only 1 recording restricted the potential of the network to become fully developed. For this particular 49 input, 3 output system, the best performance was achieved with 45 hidden nodes, and a training period of 3000 epochs.

## Chapter 7

### 7 Conclusion

An electronic nose was created to analyze high concentration alcoholic beverages. The lab bench prototype featured an array of 12 MOS sensors that were commercially available from Figaro Engineering Inc. and FiS Inc. The sample delivery method developed used a vial heating chamber that had a manual valve to allow for the operator to control the sample testing environment. The heater chamber was able to reach temperatures of 89°C and would allow for 2mL target vials to be easily interchanged for analysis. Compressed air was used to clear the chamber between samples which took approximately 30 minutes using a low air flow rate.

Previous experiments conducted from other researchers have shown the effectiveness of using a neural network to classify many other foods and beverages. These classifiers often could obtain a successful classification over 90% of the time. There have been few attempts to classify high concentration spirits, but successful devices exist to analyze wines, and beer.

Multiple experiments were created to focus on classifying 5  $\mu$ L samples of 20% Ethanol ABV, Pure Ethyl Acetate, and 99% Isopropyl Alcohol in various mixtures. Over 300 samples were collected using various methods, concentrations, sensor resistor values, and sample sizes. Multiple experiments were trialed to attempt to maximize sample collection consistency and repeatability. There were 25 samples with common collection methods that were used for feature extraction and classification. Seven different features were acquired from each of the 7 sensors used inside the chamber to create a 49 input array for a back propagating neural network used for classification. The output array consisted of 3 nodes that indicated the amount of  $\mu$ L the sample was composed of.

By stepping through iterations of various architecture designs, a 45 hidden node network was chosen as the optimal design because it had the lowest average classification error. A total of 100 randomized tests were performed on the network as it was trained for each 1000, 2000 and 3000 epochs to determine the preferred training length. As expected, the longer the network was trained, the better the overall performance was when classifying the random samples. The randomization of samples did allow for new samples to be tested which were not trained and this would increase the error upon classification. The samples recorded suffered from a floating baseline when being logged for analysis and the network was still able to produce respectable results. The 45 hidden node architecture trained for 3000 epochs was able to successfully classify samples to within 12.5% error on average.

## **7.1 Future Work**

There exist many modifications and experiments that could be trialed to potentially improve results. A larger database of samples and multiple attempts of each sample configuration would help train the network. The floating baseline on the electronic nose could be further investigated and the fluctuation could potentially be minimized by adding in a filter for the air entering the chamber. A larger array of features could be extracted from the samples collected and used as additional inputs into the neural network. Secondly, the features that are currently being used in the network may potentially be redundant or not useful. An investigation on the current features should be considered to optimize the inputs for network training and for classification. The final classification result from the neural network could potentially be used in a fuzzy classifier to match the output to one of the chemical configurations that was used.

## Bibliography

- [1] Parliament of Canada Committee Report, "Food Supply Chain - Beverage Sector," April 2013. [Online]. Available: <http://www.parl.gc.ca/HousePublications/Publication.aspx?DocId=6226525&Language=e&Mode=1&Parl=41&Ses=1&File=141>. [Accessed 12 December 2013].
- [2] M. K., C. J. van Wyk, P. Brunerie, O. P. Augustrn and A. Rapp, "Flavour Components of Whiskey. III Ageing changes in the Low-Volatility Fraction," *South African Journal for Enology and Viticulture (S AFR J ENOL VITIC)*, vol. 22, no. 2, 2001.
- [3] A. E. Laher, L. N. Goldstein, M. D. Wells, N. Dufourq and P. Moodley, "Unwell after drinking homemade alcohol – A case," *African Journal of Emergency Medicine*, vol. 3, no. 2, pp. 71-74, 2013.
- [4] R. Muresan and N. Muresan, "ELECTRONIC NOSE APPARATUS". United States of America Patent 20130061692A1, 14 March 2013.
- [5] B. P. N. Gardner J W, *Electronic Noses: Principles and Applications*, Oxford: Oxford University Press, 1999.
- [6] B. G.-S. B. Debska, "Application of artificial neural network in food classification," *Analytica Chimica Acta*, pp. 283-291, 2011.
- [7] S. P. S. M. Sindhuja Sankaran, "Olfactory receptor based piezoelectric biosensors for



detection of alcohols related to food safety applications," *Sensors and Actuators B: Chemical*, pp. 8-18, 2011.

[8] S. P. C. L. H. G. M. M. S. Balasubramanian, "Neural networks-integrated metal oxide-based artificial olfactory system for meat spoilage identification," *Journal of Food Engineering*, pp. 91-98, 2009.

[9] D. Lieberman, *The Evolution of the Human Head*, Cambridge: Harvard University Press, 2011.

[1 Y. S. Kim, S.-C. Ha, Y. Yang, Y. J. Kim, S. M. Cho, H. Yang and Y. T. Kim, "Portable  
0] electronic nose system based on the carbon black–polymer composite sensor array," *Sensors and Actuators B: Chemical*, vol. 108, no. 1, pp. 285-291, 2005.

[1 I. Campbell, "Scotch Whisky," [Online]. Available:  
1] <http://web.sls.hw.ac.uk/teaching/distilling/files/documents/IntroductionToScotchWhisky.pdf>.  
[Accessed 12 December 2013].

[1 ScotchWhisky, "Tasting Whisky," [Online]. Available:  
2] [http://www.scotchwhisky.com/english/tasting/how\\_to/tasproc.htm](http://www.scotchwhisky.com/english/tasting/how_to/tasproc.htm). [Accessed 11 December 2013].

[1 A. Lascelles, "How to Taste Whisky," *The Whisky Club*, 16 July 2013. [Online]. Available:  
3] <http://www.timeswhiskyclub.com/Blog/post/2013/07/16/How-to-Taste-Whisky.aspx>.  
[Accessed 12 December 2013].

[1 ScienceLab, "Material Safety Data Sheet Ethyl alcohol 200 Proof MSDS," 22 May 2013.

4] [Online]. Available: <http://www.sciencelab.com/msds.php?msdsId=9923955>. [Accessed 11 December 2013].

[1 ScienceLab, "Material Safety Data Sheet Ethyl acetate MSDS," 22 May 2013. [Online].  
5] Available: <http://www.sciencelab.com/msds.php?msdsId=9927165>. [Accessed 11 December 2013].

[1 ScienceLab, "Material Safety Data Sheet Ethyl Butyrate MSDS," 22 May 2013. [Online].  
6] Available: <http://www.sciencelab.com/msds.php?msdsId=9923963>. [Accessed 11 December 2013].

[1 ScienceLab, "Material Safety Data Sheet Propylene glycol MSDS," 22 May 2013. [Online].  
7] Available: <http://www.sciencelab.com/msds.php?msdsId=9927239>. [Accessed 11 December 2013].

[1 ScienceLab, "Material Safety Data Sheet Vanillin MSDS," 22 May 2013. [Online].  
8] Available: <http://www.sciencelab.com/msds.php?msdsId=9927641>. [Accessed 11 December 2013].

[1 ScienceLab, "Material Safety Data Sheet Isopropyl alcohol MSDS," 22 May 2013. [Online].  
9] Available: <http://www.sciencelab.com/msds.php?msdsId=9924412>. [Accessed 11 December 2013].

[2 A. D. Wilson and M. Baietto, "Applications and Advances in Electronic-Nose Technologies,"  
0] *Sensors*, vol. 9, no. 7, pp. 5099-5148, 2009.

[2 R. Chutia and M. Bhuyan, "Study of Temperature Modulated Tin Oxide Gas Sensor and

- 1] Identification of Chemicals," in *Computational Intelligence and Signal Processing (CISP)*, Assam, 2012.
- [2 FiS Inc., "FIS Gas Sensor SB-15 for LP-GAS (Propane/Butane) Detection," FiS Inc, Itami, 2] 1999.
- [2 Figaro USA, Inc., "TGS 2610 - for the detection of LP Gas," February 2005. [Online]. 3] Available: <http://www.figarosensor.com/products/2610pdf.pdf>. [Accessed 12 December 2013].
- [2 R. P. Lippmann, "An Introduction to Computing with Neural Nets," *ASSP Magazine, IEEE*, 4] vol. 4, no. 2, pp. 4-22, 1987.
- [2 C. P. Tim, S. S. Susan, T. N. H. and W. G. J., *Handbook of Machine Olfaction: Electronic 5] Nose Technologies*, WILEY-VCH, 2003.
- [2 K. T. S. C. S. Y. C. K. L.C. Wang, "A bio-inspired two-layer multiple-walled carbon 6] nanotube–polymer composite sensor array and a bio-inspired fast-adaptive readout circuit for a portable electronic nose," *Biosensors and Bioelectronics*, pp. 4301-4307, 2011.
- [2 K. L. Priddy and P. E. Keller, *Artificial Neural Networks An Introduction*, Bellingham: The 7] International Society for Optical Engineering, 2005.
- [2 H. Yonaba, F. Anctil and V. Fortin, "Comparing Sigmoid Transfer Functions for Neural 8] Network Multistep Ahead Streamflow Forecasting," *Journal of Hydrologic Engineering*, vol. 15, no. 4, pp. 275-283, 2010.

- [2 U. Siripatrawan, J. E. Linz and B. R. Harte, "Electronic sensor array coupled with artificial neural network for detection of Salmonella Typhimurium," *Sensors and Actuators*, vol. 119, pp. 64-69, 2006.
- [3 J. G. R. Menzel, "Gradient gas sensor microarrays for on-line process control — a new dynamic classification model for fast and reliable air quality assessment," *Sensors and Actuators*, vol. B, no. 68, pp. 115-122, 2000.
- [3 A. Tripathy, A. K. Mohanty and M. N. Mohanty, "Electronic Nose for Black Tea Quality Evaluation Using Kernel Based Clustering Approach," *International Journal of Image Processing (IJIP)*, vol. 6, no. 2, pp. 86-93, 2012.
- [3 V. Gupta and K. Gupta, "Electronic Odour Measurement and Sensing using E-Nose," *International Journal of Scientific & Engineering Research*, vol. 4, no. 2, pp. 1-9, 2013.
- [3 N.-J. Huan and R. Palaniappan, "Neural network classification of autoregressive features from electroencephalogram signals for brain-computer interface design," *Journal of Neural Engineering*, vol. 1, no. 3, pp. 142-150, 2004.
- [3 Y. H. Tay and M. Khalid, "Comparison Of Fuzzy Artmap And MLP Neural Networks For Hand-Written Character Recognition," in *Pre-prints of International Federation of Automatic Control (IFAC) Symposium on Artificial Intelligent in Real -Time Control*, 1997, pp. 363--37.
- [3 K. R. Kashwan and M. Bhuyan, "Robust Electronic-Nose System with Temperature and Humidity Drift Compensation for Tea and Spice Flavour Discrimination," in *2005 Asian Conference on sensors and the International Conference on New Techniques in*

*Pharmaceutical and Biomedical Research*, Malaysia, 2005.

- [3 M. Lieberman, "MOS Electronic Nose for Alcohol and Solvents with Analysis by Hilbert-6] Huang Transform," University of Guelph, Guelph, 2013.
- [3 A. Kusiak, F. Tang and G. Xu, "Multi-objective optimization of HVAC system with an 7] evolutionary," *Energy*, p. 2440–2449, May 2011.
- [3 National Semiconductor, "Precision Centigrade Temperature Sensor," National 8] Semiconductor, 4 April 2012. [Online]. Available: <http://www.national.com/mpf/LM/LM35.html#Overview>. [Accessed 4 April 2012].
- [3 A. C. F. A. T. M. J. R. Paulo Cortez, "Modeling wine preferences by data mining from 9] physicochemical properties," *Decision Support Systems*, pp. 547-553, 2009.
- [4 S. Rajasekaran and G. A. Vijayalakshmi Pai, "Simplified Fuzzy ARTMAP as Pattern 0] Recognizer," *Journal of Computing in Civil Engineering*, vol. 14, no. 2, pp. 92-99, 2000.
- [4 Hammond Manufacturing, "Hammond Manufacturing R191-170-000," [Online]. Available: 1] <http://www.hammondmfg.com/pdf/R191-170-000.pdf>. [Accessed 12 December 2013].

## Appendix A – 2D Drawings

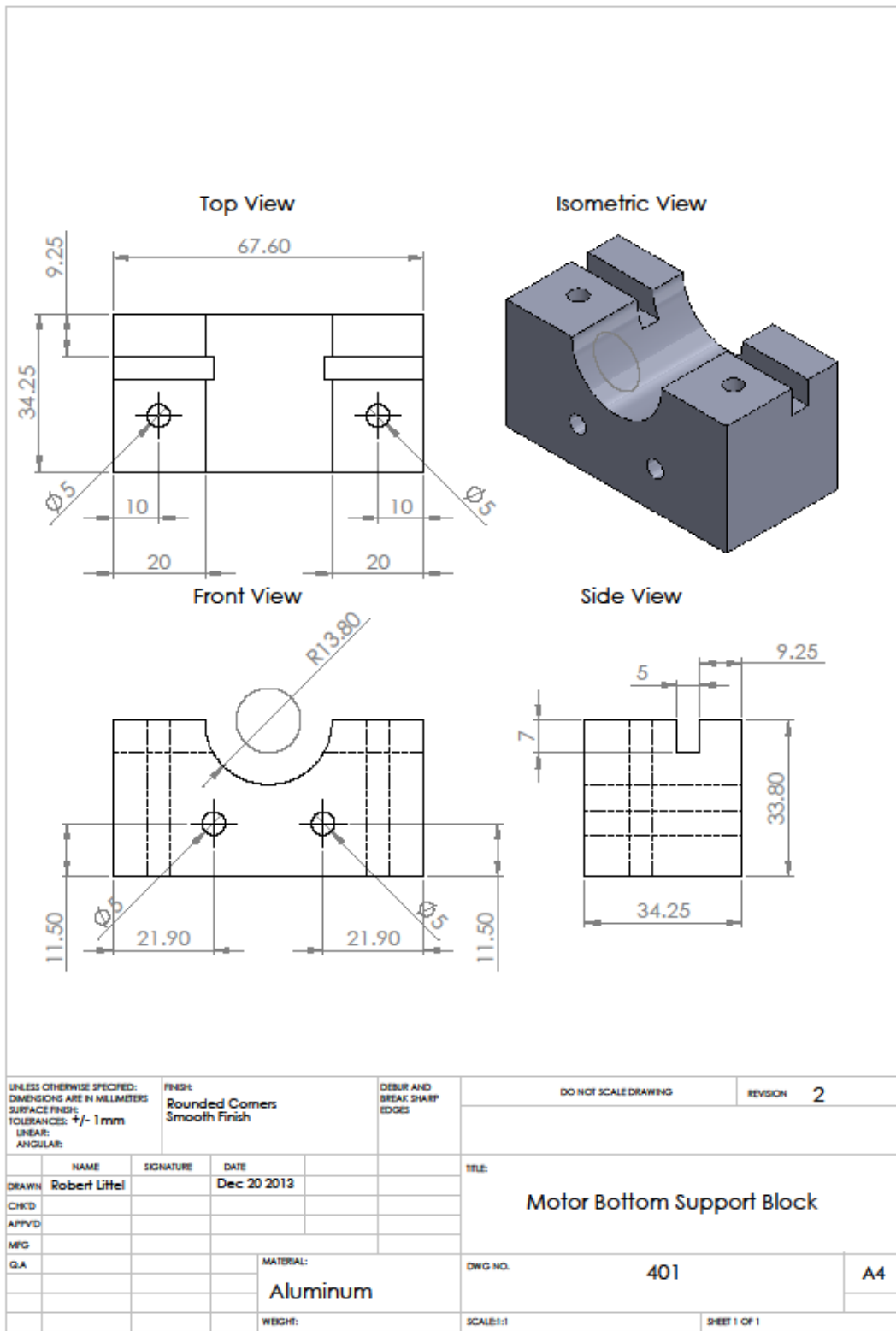


Figure 38: 2D Drawing - Motor Bottom Support Block

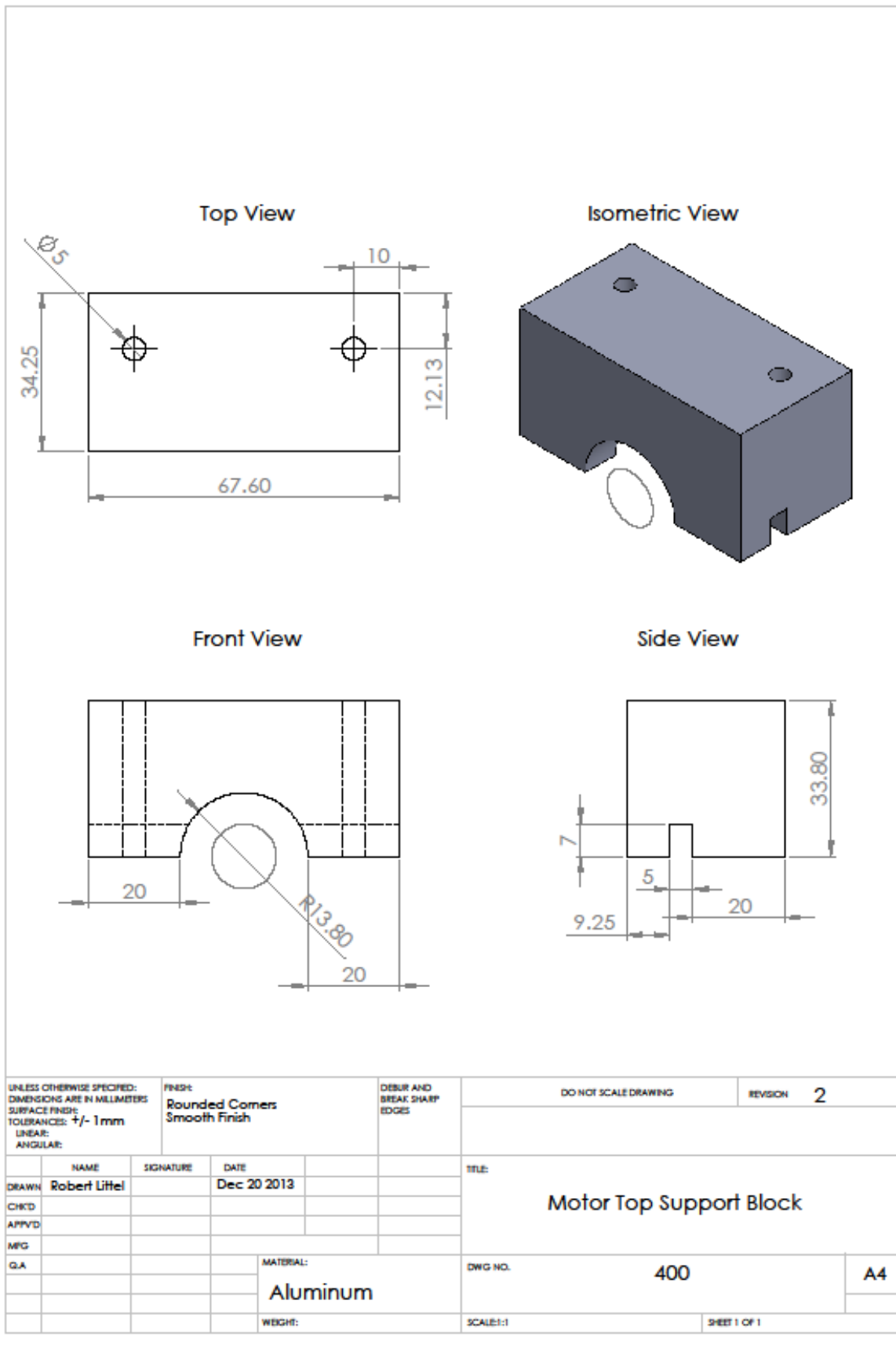
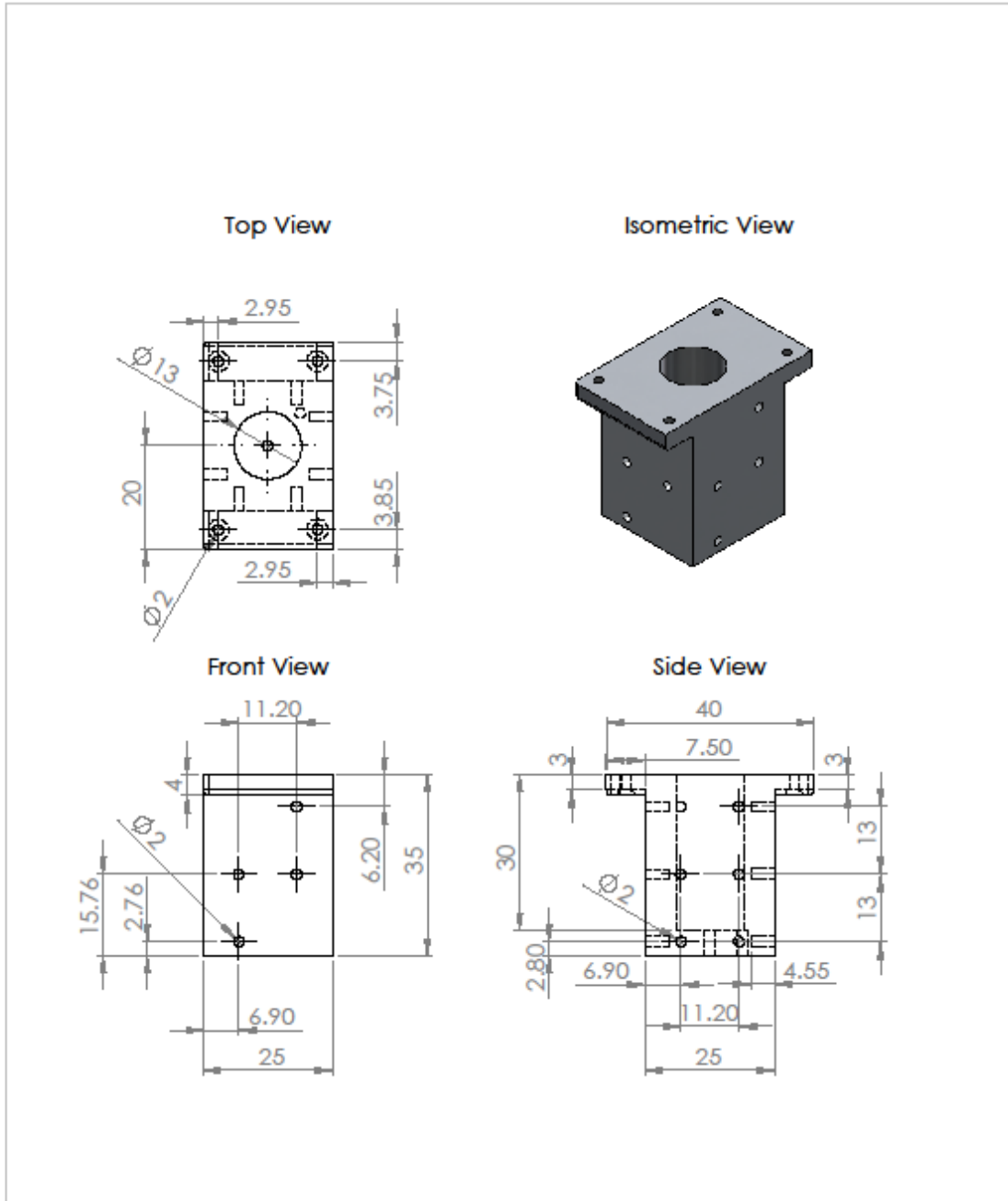


Figure 39: 2D Drawing - Motor Top Support Block



UNLESS OTHERWISE SPECIFIED: DIMENSIONS ARE IN MILLIMETERS SURFACE FINISH: TOLERANCES: +/- 1mm LINEAR: ANGULAR:				FINISH: Rounded Corners Smooth Finish		DEBUR AND BREAK SHARP EDGES		DO NOT SCALE DRAWING		REVISION 2	
								A total of 16 screw holes predrilled at the base. The base is symmetric.			
DRAWN		NAME		SIGNATURE		DATE		TITLE:			
		Robert Littel				Dec 20 2013		Vial Heater Bottom Section Block			
CHK'D											
APP'VD											
MFG											
QA								MATERIAL:		DWG NO.	
								Aluminum		350	
								WEIGHT:		SCALE:1:1	
										SHEET 1 OF 1	
										A4	

Figure 40: 2D Drawing - Vial Heater Bottom Section Block



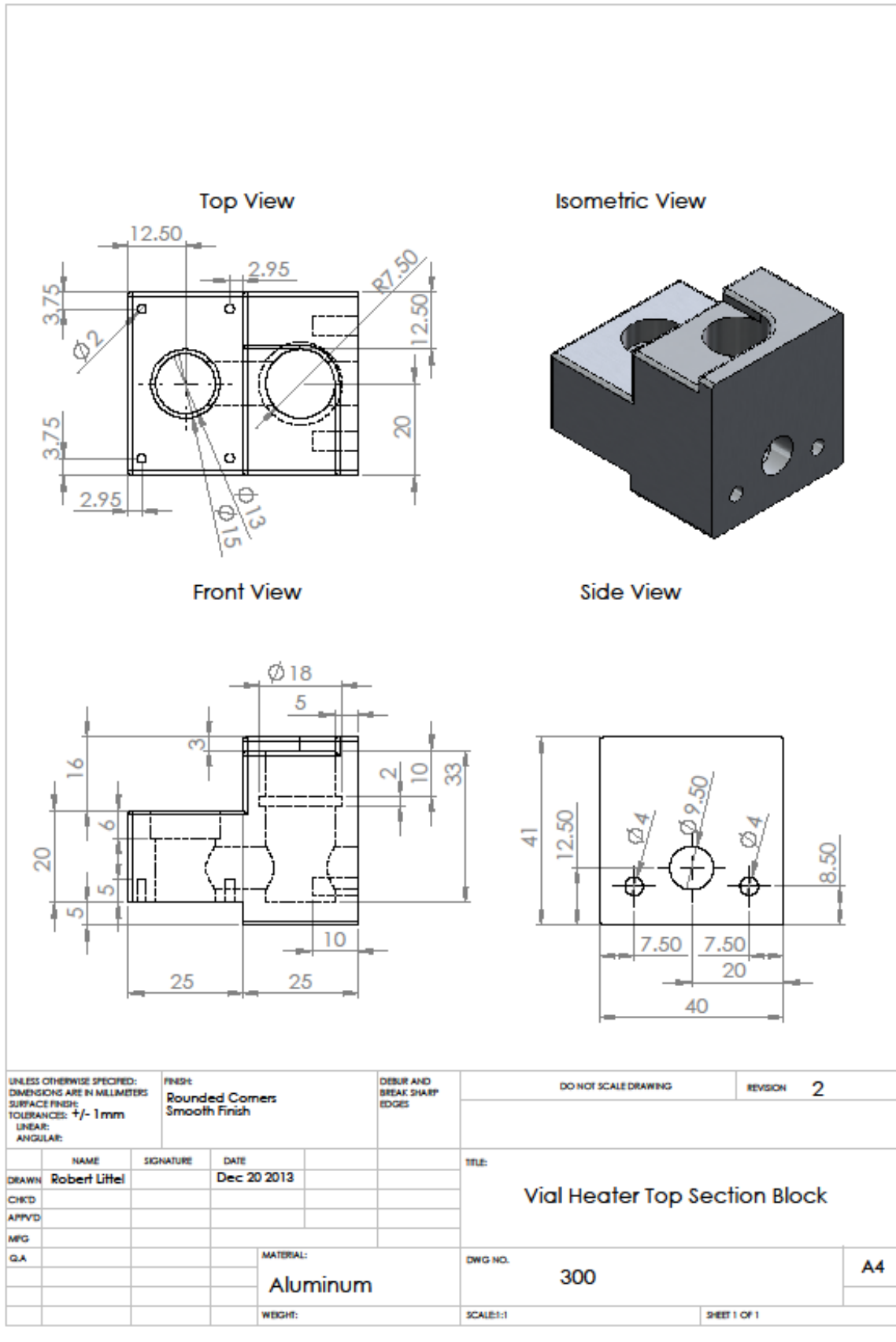


Figure 41: 2D Drawing - Vial Heater topSection Block

## Appendix B – Sample Initialization Conditions

Sensor Start Values (K $\Omega$ )							Humeral Sensors				Environment Conditions						
2	3	4	5	8	10	11	Temp 1	Temp 2	Humid 1	Humid 2	Time of Sample	Temp °C	Humidity				
<b>June 24 2013</b>																	
14.32	43.25	36.141	11.787	11.438	9.208	9.213					<b>Legend</b>						
14.259	43.755	35.636	11.806	10.998	9.053	9.299					<b>Resistor Values</b>	<b>Color Code</b>					
14.251	43.807	36.126	11.828	10.642	8.876	9.177					2499						
14.277	44.941	36.596	12.198	10.818	9.078	9.343					10000						
14.626	46.182	39.12	12.553	11.021	9.336	9.564					12000						
14.674	46.601	38.335	12.602	10.746	9.098	9.323					24900						
14.478	46.274	37.642	12.416	10.526	8.895	9.067					Invalid Data	<del>Strikethrough</del>					
14.485	46.76	37.867	12.415	10.439	8.891	9.1											
14.409	46.877	37.895	12.297	10.467	8.927	9.148											
14.556	46.614	39.603	12.42	10.642	9.103	9.288											
14.298	46.293	38.449	12.301	10.404	8.895	9.039											
<b>June 26 2013</b>																	
15.004	49.965	42.612	13.167	12.428	10.638	10.581											
14.628	49.221	41.547	13.128	11.754	8.918	10.269											
14.358	48.94	40.856	12.77	11.222	8.478	9.829											
14.587	49.291	41.062	12.942	12.21	8.413	9.79											
14.613	49.3	41.01	12.915	11.108	8.325	9.687											
14.527	49.405	40.823	12.825	10.937	8.176	9.54											
14.375	49.394	40.635	12.672	10.705	8.003	9.362											

Table 20: Sample Initialization Conditions Part 1

Sensor Start Values (K Ω)							Humeral Sensors				Environment Conditions		
2	3	4	5	8	10	11	Temp 1	Temp 2	Humid 1	Humid 2	Time of Sample	Temp °C	Humidity
<b>July 10 2013</b>													
14.029	49.608	42.587	12.131	3.74	8.915	3.358	45.3	43.9	17.6	35.3			
13.589	48.599	40.741	11.711	4.226	8.387	3.778							
13.333	47.838	39.663	11.417	4.439	8.024	3.938							
13.733	49.666	40.858	11.861	4.791	7.916	4.254	46.6	45.2	17.3	35.3			
13.69	49.86	40.989	11.663	4.934	7.916	4.373	46.7	45.3	17.2	35.3			
13.759	49.965	40.708	11.78	5.016	7.855	4.448	46.7	45.3	17.1	35.2			
13.8	50.037	40.674	11.802	5.047	7.79	4.483	46.5	45.1	17.1	35.2			
13.916	50.19	40.832	11.878	5.102	7.786	4.529	46.5	45.1	17.1	35.2			
13.98	50.318	40.866	11.94	5.165	7.795	4.587	46.4	45	17.1	35.2			
13.816	50.395	40.733	11.76	5.082	7.582	4.506	46.5	45.1	17.3	35.2			
13.969	50.731	40.991	11.94	5.22	7.736	4.638	46.4	45	17.1	35.2			
13.834	50.72	40.871	11.768	5.137	7.554	4.557	46.4	45.1	17.3	35.2			
<b>July 16 2013</b>													
13.632	51.99	43.006	11.912	11.551	8.744	10.201	44.7	43.8	19.8	34.8	15:29		
13.82	51.99	42.822	11.998	11.426	8.584	10.072	46.3	45.2	17.7	34.9	16:11		
13.831	51.889	42.548	12.037	11.115	8.342	9.807	46.7	45.6	16.9	34.9	16:57		
13.704	51.878	42.247	11.962	10.765	8.085	9.504	46.6	45.5	16.9	34.9	17:46		
13.111	49.968	38.784	11.695	10.051	4.476	7.431	45.9	46.3	20.4	34.9	9:52 PM		
12.844	49.494	38.066	11.325	9.899	7.344	8.539	46.3	46.7	20.8	34.9	10:33 PM		
12.688	49.352	37.555	11.099	9.736	7.233	8.385	46.5	46.9	21	34.9	23:13		

Table 21: Sample Initialization Conditions Part 2

Sensor Start Values (K Ω)							Humeral Sensors				Environment Conditions		
2	3	4	5	8	10	11	Temp 1	Temp 2	Humid 1	Humid 2	Time of Sample	Temp °C	Humidity
<b>July 18 2013</b>													
13.543	52.04	40.299	11.556	10.69	8.041	9.449	46.9	46	20.7	34.8	2:32 PM	32 feels like 38	63%
13.065	51.559	38.815	11.133	10.1	7.515	8.829	47.4	46.7	19.7	34.9	3:07 PM	32 feels like 40	59%
12.54	50.498	37.496	11.033	9.889	7.426	8.69	47	47.4	21.6	34.9	3:48 PM	32 feels like 41	58%
12.533	50.066	37.773	10.727	9.904	7.487	8.6	47.9	48.4	21.3	34.9	4:29 PM	33 feels like 39	58%
12.197	49.494	36.631	10.526	9.543	7.166	8.295	48.1	48.6	21.9	34.9	5:03 PM	32 feels like 40	58%
12.053	49.316	36.251	10.412	9.254	6.972	8.132	47.8	48.4	22.5	34.9	5:51 PM	32 feels like 40	58%
12.037	49.341	36.69	10.226	9.264	7.008	8.004	47.9	48.4	22.6	34.9	6:28 PM	32 feels like 39	58%
12.28	50.095	36.917	10.706	9.174	6.86	8.088	47.4	47.8	22.1	34.9	20:23	29 feels like 37	58%
12.571	50.143	37.205	10.821	9.425	7.12	8.292	47.2	47.7	22.5	34.9	9:07 PM	28 feels like 37	64%
12.575	50.292	37.676	10.581	9.449	7.186	8.166	47.2	47.7	22.5	34.9	9:40 PM	28 feels like 37	70%
12.535	50.311	37.191	10.692	9.366	7.069	8.132	47.2	47.6	22.5	34.9	10:10 PM	27 feels like 37	74%
<b>July 19 2013</b>													
13.015	51.598	39.064	11.174	9.955	7.679	8.8	45.7	45.9	25.1	34.7	12:01 PM	31 feels like 40	57%
13.16	51.709	39.006	11.303	10.016	7.679	8.788	47	47.4	22.4	34.8	12:41 PM	31 feels like 41	57%
13.242	51.732	38.938	11.349	9.953	7.647	8.79	47.5	47.8	21.2	34.8	1:22 PM	31 feels like 39	54%
13.245	51.69	38.72	11.349	9.867	7.563	8.692	47.6	47.9	20.9	34.8	2:05 PM	30 feels like 41	63%
13.308	51.693	38.703	11.412	9.838	7.544	8.662	47.5	47.9	20.8	34.8	2:41 PM	32 feels like 42	54%
13.252	51.686	38.591	11.41	9.781	7.45	8.588	47.5	47.9	20.8	34.8	3:22 PM	32 feels like 41	50%
13.205	51.579	38.345	11.328	9.672	7.383	8.513	47.6	47.9	20.8	34.8	4:03 PM	32 feels like 41	50%
13.227	51.655	38.319	11.361	9.642	7.359	8.491	47.6	47.9	20.7	34.8	4:41 PM	32 feels like 41	50%
12.964	51.533	37.777	11.167	9.432	7.151	8.254	47.6	47.9	20.6	34.8	5:17 PM	33 feels like 41	46%
12.996	51.724	37.892	11.229	9.378	7.099	8.252	47.2	47.6	20.9	34.8	18:12	25 feels like 34	82%

Table 22: Sample Initialization Conditions Part 3